Oligomeric Ionic Liquids: Bulk, Interface and Electrochemical Application in Energy Storage

Dan-Dan Li

Xiang-Yu Ji

Ming Chen

Yan-Ru Yang

Xiao-Dong Wang
1. State Key Laboratory of Alternate Electrical Power System with Renewable Energy Sources, North China Electric Power University, Beijing 102206, China;2. Research Center of Engineering Thermophysics, North China Electric Power University, Beijing 102206, China;, wangxd99@gmail.com

Guang Feng
3. State Key Laboratory of Coal Combustion, School of Energy and Power Engineering, Huazhong University of Science and Technology (HUST), Wuhan 430074, China;, gfeng@hust.edu.cn

Oligomeric Ionic Liquids: Bulk, Interface and Electrochemical Application in Energy Storage

Dan-Dan Li[1,2], Xiang-Yu Ji[3], Ming Chen[3], Yan-Ru Yang[1,2],

Xiao-Dong Wang[1,2*], Guang Feng[3*]

(*1. State Key Laboratory of Alternate Electrical Power System with Renewable Energy Sources,*
North China Electric Power University, Beijing 102206, China; 2. Research Center of
Engineering Thermophysics, North China Electric Power University, Beijing 102206, China;
3. State Key Laboratory of Coal Combustion, School of Energy and Power Engineering,
Huazhong University of Science and Technology (HUST), Wuhan 430074, China)

Abstract: Over recent years, oligomer ionic liquids (OILs), a novel class of ionic liquids, are becoming preferential electrolytes for high-performance energy-storage devices, such as supercapacitors with enhanced energy density and non-flammable lithium-ion batteries (LIBs). Herein, structures, properties, and their associations of the up-to-the-minute formulated OILs are systematically summarized and elaborately interpreted, especially for dicationic ionic liquids and tricationic ionic liquids. The physicochemical and electrochemical properties of OIL-based electrolytes are presented and analyzed, which are vitally important for supercapacitors and LIBs. Subsequently, the applications of OILs as electrolytes for supercapacitors and LIBs are summarized, with the comparisons of the energy-storage mechanisms and performance between OILs and MILs electrolytes in supercapacitors. Meanwhile, the optimization of the dynamic performance of OILs electrolytes is provided. Finally, the main difficulties and probable perspectives of OIL-based electrolytes are presented for future work. This review would contribute to a deep understanding of OILs and design optimized OIL-based electrolytes for energy storage systems.

Key words: oligomer ionic liquids; properties and structures; supercapacitors; lithium-ion batteries

1 Introduction

The development of efficient electric energy storage with high energy/power density, good safety, and long lifetime plays an indispensable role in the utilization of renewable and clean energy resources[1-3]. Among the energy storage solutions, lithium-ion batteries (LIBs) and supercapacitors have drawn much attention[4, 5]. LIBs are characterized by long discharge life, high operating voltage, high specific energy, and low environmental pollution. Hence, they have gradually become the main power source for electric vehicles with low-carbon even zero-carbon emissions[6-8]. However, the potential inflammation risks of organic electrolytes and the moderate power density cause a negative consequence that LIBs fail to satisfy safe and more rapid energy needs in production and life[9-14]. Luckily, supercapacitors can achieve the rapid charge-discharge process by reversible charge adsorption and desorption on the electrodes rather than the chemical reaction. Thus, they own the ultrahigh power density, good safety performance, and long cycle life, which allows supercapacitors to be used as paral-

leling devices of LIBs to gain high-capacity and high-power density electric energy storage systems[12, 15-17]. In addition, supercapacitors have been applied individually in many fields, including the national defense and military industry, aerospace, smart grid, electronic information, and industrial production[18-20]. However, the broad availability is confined by the limited energy density[21, 22]. As electrolytes are one of the vital constituents of supercapacitors and LIBs, the selection and development of high-performance electrolytes have been one of the ways to solve the above disadvantages[23, 24].

In the past several decades, room temperature ionic liquids (ILs), known as following monocationic ionic liquids (MILs), on account of their glamorous qualities, including wider potential and temperature windows, greater thermostability, non-flammability, lower vapor pressure, compared with aqueous and organic electrolytes, are deemed as a kind of distinguished electrolytes for supercapacitors and LIBs[25, 26]. So far, MILs-based supercapacitors and LIBs have been extensively researched by theoretical, experimental, and modeling methods. The elevated energy density in supercapacitors and the high safety performance of LIBs could be observed[27-30]. Remarkably, these works have been systematically reviewed by prominent researchers[31, 32]. In the latest few years, in parallel with research into MILs, a new line of interest in dicationic ionic liquids (DILs), tricationic ionic liquids (TILs), tetracation ILs, and poly(ionic liquid)s (PILs) has appeared[33-46]. Among these ILs, PILs are solid polyelectrolytes including multiple duplicate cation or anion monomers together with a polymeric backbone[47, 48]. With the increased need for wearable electronic devices, PILs-based electrolytes become the most promising candidate for flexible and lightweight supercapacitors and LIBs. This is because that PILs electrolytes display greater adjustability, excellent conduction of electricity, and adequate compatibility with electrodes, compared with common polyelectrolytes. Reviews focusing on the synthetic strategies, chemical structures, physical properties, and applications of PILs have been published

recently[48-50]. However, there is no systematic review concerning on DILs, TILs, and tetracation ILs. These ILs can be termed as oligomer ionic liquids (OILs), an intermediate state between low-molecular-weight MILs and macromolecular-state PILs[50]. They are composed of several positively charged heads (such as imidazolium, pyrrolidonium, and ammonium groups) and spacer bridges connecting the heads (such as alkyl-based and ether-based chains) in a cation and matching anions (e.g., Br^-, BF_4^-, PF_6^-, and Tf_2N^-, etc.). OILs are considered the evolution of MILs and own more excellent properties, including a larger liquid temperature range, higher thermal stabilities, widened voltage windows (4.3 ~ 6 V), and greater flexibility[33, 44-46, 51, 52]. For this reason, OILs as electrolytes have been brought into noteworthy focus in supercapacitors and LIBs[53-60], as shown in Figure 1. However, OILs have higher viscosity due to stronger charged heads-anions interactions in contrast to MILs, which significantly hinders ionic transportation and wrecks the power densities of supercapacitors and LIBs. Hence, it is very important to concentrate on declining their viscosities. In contrast to the experimental method, the model studies can offer more profound molecular insights into the microstructures and properties of OILs. In this review, by focusing on OILs, especially DILs and TILs, the relationships between various structures and physical chemistry properties of OILs in model studies are generalized and compared with the corresponding MILs to design optimized OILs electrolytes for energy storage equipment. Special attention is paid on the structures and performance of the OIL-based interfaces, and the recent development of supercapacitors and LIBs with OILs electrolytes. Furthermore, the challenges and potential prospect forecasts of OILs are discussed.

2 Properties of Bulk OILs

2.1 Molecular Simulation Setup for OILs

The diverse combinations of multications and anions bring up the flexible structures and tunable properties of OILs for the designated requests. However, It is nearly impossible to sift out satisfactory OILs among thousands of combinations by human instinct
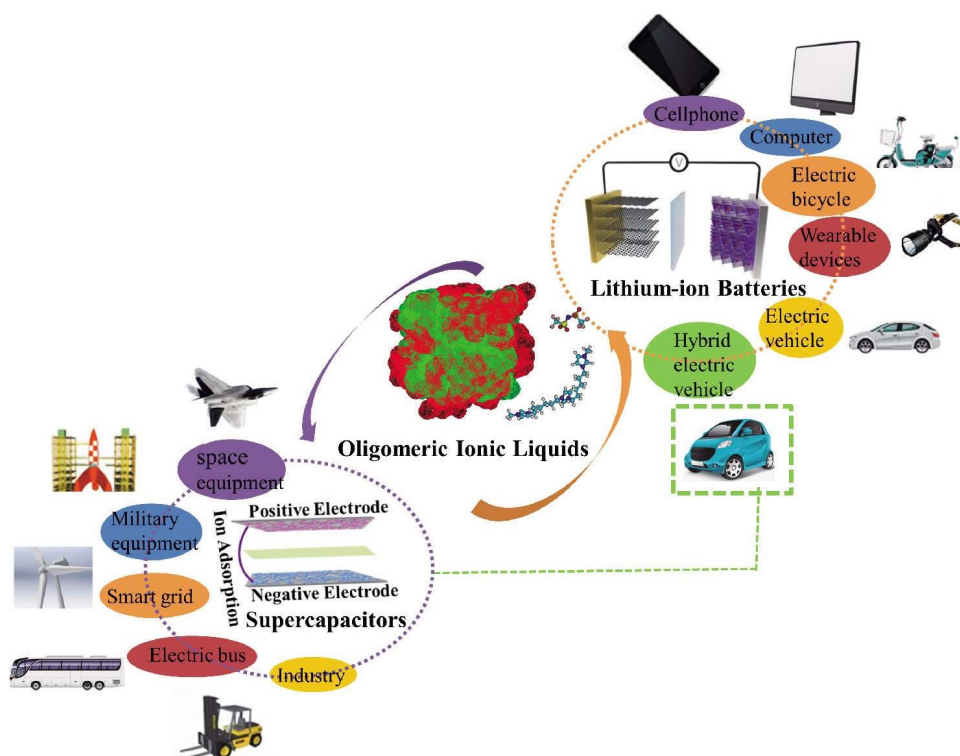
Figure 1 Applications of OIL-based electrolytes in electric energy storage devices. Reproduced with permission of Ref. 8, Copyright 2021, Elsevier. (color on line)

through the traditional guess-and-check method[33, 45]. With the aid of the development of atomistic simulation, a reliable interpretation of the relationship between the structure and the properties has been provided via the theoretical simulation method, such as density functional theory (DFT) and molecular dynamic (MD) simulations. DFT, the method of studying electronic structures for multi-electron systems, has been widely applied to explore the electronic properties and structures of OILs[60-63]. Firstly, the optimization of the individual cation and anion in the initial structures of OILs is conducted to gain the bond, angle and torsion angle between atoms in the most stable ion, and the integrated geometry optimization and the evaluation of electronic properties of the ion pairs are carried out, based on the gained optimized ion structures. The following computation of the frequency for the optimized geometry structure is implemented to guarantee a minimum potential energy surface and cation-anion hydrogen bonds are evaluated. In the end, the interactions between ions

and structural properties can be computed using the related theory and the structures of liquid OILs will be researched, according to these properties.

In parallel, MD simulation has become a powerful tool to estimate the microstructures and properties of ILs from a micro viewpoint. In principle, the Newton equation is solved to determine the evolution of positions and momentum of each atom over time. By taking the average of the microstates over time, thereby, the macroscopic properties of the system (including pressure, energy, diffusion coefficient, and viscosity), and the microstructure, such as the spatial distribution of atoms are derived. However, the reliability of the simulation results relies on the precision of force fields, which can properly regenerate experimental characteristics. The non-polarized force field established by Canongia Lopes and Padua has been broadly employed for MILs and is evolved by simply modifying the charges of the individual atoms in the spacers to be utilized well in OILs systems[59, 64-66]. Although the static properties are modelled precisely, dynamic
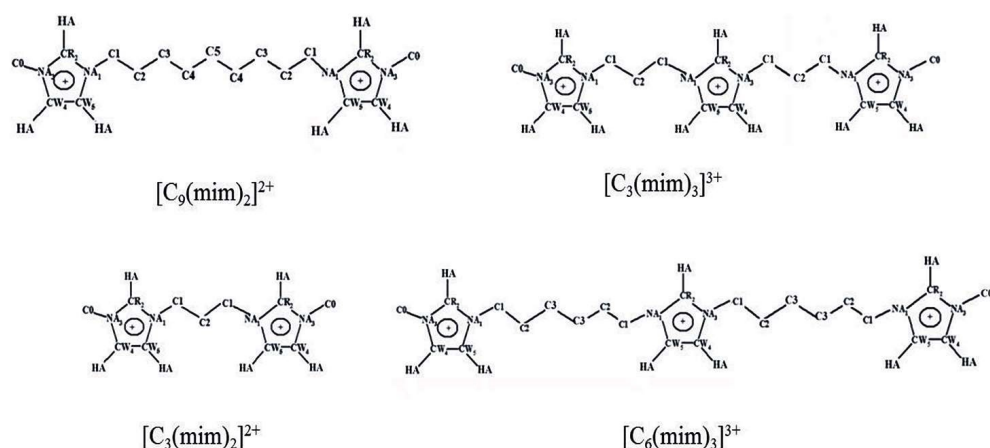
Figure 2 The molecular structures of cations in the common DILs and TILs.

Table 1 Scaled atomic charges and Lennard-Jones parameters of cations in common DILs and TILs[56, 59, 66].

Atom	Charge (e)				L-J parameter	
	$[C_3(mim)_2]^{2+}$	$[C_9(mim)^2]^{2+}$	$[C_3(mim)_3]^{3+}$	$[C_6(mim)_3]^{3+}$	σ^{ii} (Å)	ε^{ii} (kJ·mol^{-1})
NA1	0.12	0.12	0.12	0.12	3.25	0.71128
CR2	-0.088	-0.088	-0.088	-0.088	3.55	0.29288
NA3	0.12	0.12	0.12	0.12	3.25	0.71128
CW4	-0.104	-0.104	-0.104	-0.104	3.55	0.29288
CW5	-0.104	-0.104	-0.104	-0.104	3.55	0.29288
C0	-0.136	-0.136	-0.136	-0.136	3.5	0.27614
C1	-0.136	-0.136	-0.136	-0.136	3.5	0.27614
C2	0.008	0.008	0.008	0.008	3.5	0.27614
C3		-0.096		-0.096	3.5	0.27614
C4		-0.096		-0.096	3.5	0.27614
C5		-0.096		-0.096	3.5	0.27614
H0	0.104	0.104	0.104	0.104	2.5	0.12552
H1	0.104	0.104	0.104	0.104	2.5	0.12552
H2	0.100	0.048	0.100	0.048	2.5	0.12552
H3		0.048		0.048	2.5	0.12552
H4		0.048		0.048	2.5	0.12552
H5		0.048		0.048	2.5	0.12552
HA	0.168	0.168	0.168	0.168	2.42	0.12552

properties are greatly underestimated for high-viscosity OILs. In contrast, the polarizable one is more useful for predicting the dynamic properties of ILs. Nevertheless, it is not appropriate for OILs with numerous particles because of the extremely high computa-

tional cost[67]. As a result, to optimize the non-polarized force fields for OILs, a scaling factor is introduced to weaken the electrostatic interaction between ions by scaling down each atom charge of OILs, which has been proved to be a capable way of repro-

ducing experimental dynamic properties[61, 67]. The detailed scaled atomic charges and Lennard-Jones parameters of cations in the common DILs and TILs are summarized in Table 1.

2.2 Relationship between Physical/Electrochemical Properties and Ion Structures of OILs

Compared with MILs, the cation of OIL is composed of terminal chains, several positively charged heads and spacer bridges connecting the heads. Consequently, these unique structures generate symmetric or asymmetric configurations, thereby, leading to designable physical chemistry properties. Due to the designability of OILs, much effort has been devoted to the study of the relationship between properties and multicationic or anionic structures via MD simulations and DFT methods. Some typical molecular structures of cations and anions in the common OILs are shown in Figure 3.

Density, as one of the fundamental properties of OILs, has been widely investigated via theoretical simulations. It was found that the density of the imidazolium- and ammonium-based DILs is larger than that of the MIL $[C_5mim][Tf_2N]$ but is lower than that of the corresponding symmetric DIL $[C_5(mim)_2][Tf_2N]_2$,

which may be ascribed to the greater cations-anions associations in $[C_5(tma)(mim)][Tf_2N]_2$[68]. When referring to the linker length, MD simulations demonstrated that the density of DILs would decrease as the linker length between rings increases[61, 69]. Except for the charged rings and spacers, the structures of dications are revealed to be affected by the terminal chains, resulting in different densities. MD simulations of $[C_n(amim)_2][Tf_2N]_2$ (n = 2, 4, 6) testify that the introduction of the amide group in the terminal alkyl chains makes densities greater, on account of the more intense cations-anions interactions[70]. In summary, there is a reasonable connection between the densities of DILs and dications-anions associations. Furthermore, the role of the anionic characteristics has been also studied for DILs comprised of the cation $[C_n(mim)_2]^{2+}$ (n = 3, 6, and 9) and two homoanions ($[Br^-]$, $[BF_4^-]$, and $[PF_6^-]$). It is inferred that the density value is inversely proportional to the anion weight with the same dication[69], which completely matches the tendency obtained in MILs simulations[71, 72].

In addition, it is known that the power density of energy storage systems with OILs electrolytes depends on the rate of the ionic migration toward the electrodes. Thus, some MD studies have been devot-

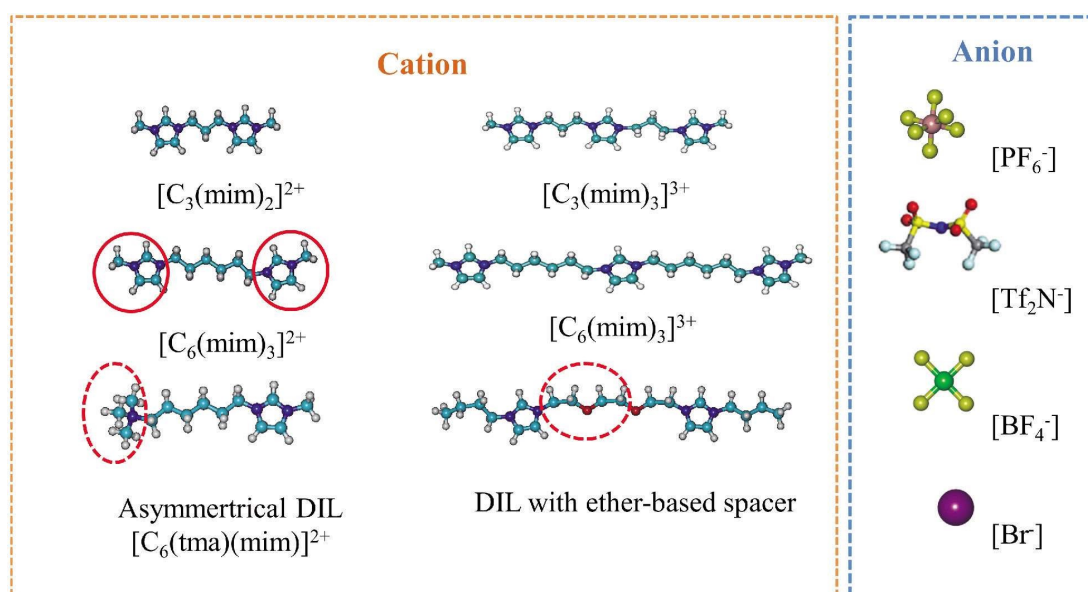

Figure 3 The molecular structures of cations and anions in the common OILs. The red circles denote the imidazolium ring, ammonium-based charged head, and the ether-based spacer of dications, respectively. (color on line)

ed to exploring the relations between ionic structure and dynamic performance. According to the calcula tion results, it was found that the charged heads in the dications have a significant impact on ionic migration. For instance, the diimidazolium DILs diffuse faster than dipyrrolidinium-based DILs due to the two-dimensional configuration of the imidazolium rings[73]. Furthermore, the dynamic behavior of dications in DILs with anions $[PF_6^-]$, $[Tf_2N^-]$, or $[Br^-]$ exhibits a similar tendency in which the ionic velocity slows down as the spacer length increases. Meanwhile, the ion diffusion coefficient in DILs lowers an order of magnitude when compared to MILs[61, 74, 75]. Unexpectedly, the diffusion of $[C_n(mim)_2]^{2+}$ in DILs with $[BF_4^-]$ displays diverse tendency: $[C_6(mim)_2]^{2+} > [C_9(mim)_2]^{2+} > [C_3(mim)_2]^{2+}$, indicating a counterbalancing between the spacer length and anionic characteristic contributing to the diffusion behavior of dications[61]. In addition, the spacer linker held by the two charged heads diffuses faster than the heads in a relatively short period, and the ether groups instead of the —CH_2— units in spacers can remarkably reduce the viscosities of DILs, promoting ionic velocity[60].

The obtained density, viscosity values, and the relationships between the properties of OILs and dicationic and anionic structures from MD simulations are exactly in line with information in experiments, as shown in Table 2 in which we have comprehensively summarized some important properties of all available DILs, including molar mass, melting point, thermal decomposing temperature, density, viscosity, solution in water and organic solvent, and electrochemical window.

The TILs, composed of three positively charged heads and spacers connecting the heads linearly or triangularly, can be divided into trigeminal TILs (TTILs) and linear TILs (LTILs) based on their different geometric structures[44-46]. In contrast to DILs, the theoretical work on TILs and tetracation ILs by MD simulations or DFT methods are still scarce. More recently, Moosavi et al.[67] firstly provided evidence that the temperature and the length of the —CH_2— unitbased spacer have a noteworthy effect on the den-

sities of room temperature LTILs $[C_n(mim)_3][Tf_2N]_3$ (n = 3, 6, 10) by MD simulations. The densities of LTILs are greater than those of MILs and DILs with the same anions $[Tf_2N^-]$ and the same rule that the density declines as temperature and the spacer length increase is obtained[68, 79]. As for TTILs, though they have similar densities to LTILs, it was found that the length of the spacer has no significant effect on the densities of TTILs[45]. Furthermore, the simulations of the same LTILs are carried out, using the modified non-polarized force field. As expected, the density values calculated in our simulations agree with the simulation by Moosavi et al.[80].

The ionic migration of LTILs is greatly slower than those of MILs and DILs due to the comparable viscosities[67]. Interestingly, different from the trend observed in $[Tf_2N^-]$-based MILs and DILs that the ionic diffusion coefficient increases with the extending linker length, the diffusion coefficient of $[C_n(mim)_3]^{3+}$ in LTILs follows this order: $[C_6(mim)_3][Tf_2N]_3 > [C_3(mim)_3][Tf_2N]_3 > [C_{10}(mim)_3][Tf_2N]_3$, which is coincident with the change of the viscosity in the experiment[45]. The change in the viscosity results from a com promise between the weakened cations-anions correlations and enhanced spacer linkers-ions van der Waals interactions as the linker length extends. In addition, the diffusion ability of different groups such as the spacer linkers, and the charged heads have been explored by MSD, these results indicate that the tricationic structure featured with tightly interlinking groups allows each group to exhibit an approximate diffusion rate.

In addition, the electrochemical stabilities of OILs-based electrolytes play a vital role in supercapacitors and LIBs. The important property is expressed by the width of the electrochemical window (ECW) depending on the resistances of reduction and oxidation of counterions on the electrodes[78]. Little data available from experiments in Table 2 and Table 3 indicates that like PILs, the ECW of OILs varies widely and fails to rank below the corresponding MILs. Moreover, it is tested that the electrochemical stabilities of the pyrrolidonium-based OILs are more excellent

Table 2 Physiochemical and electrochemical properties of dicationic ionic liquids[33-43, 76-78].

Physicochemical Properties of Symmetrical Imidazolium and Pyrrolidinium DILs								
Ionic liquid	M_w (g·mol^{-1})	MP(℃)	T_d(℃)	Density (g·cm^{-3})	Viscosity	Miscibility[a]		ECW (V)
						water	ACN	
[C$_3$(mim)$_2$][Br]$_2$	366.10	162	288			M	I	
[C$_3$(mim)$_2$][Tf$_2$N]$_2$	766.58	−4	401	1.61	249 cP	I	M	
[C$_3$(mim)$_2$][BF$_4$]$_2$	379.90	117				M	M	
[C$_3$(mim)$_2$][PF$_6$]$_2$	496.22	131	320			I	M	
[C$_6$(mim)$_2$][Br]$_2$	408.18	155	298			M	I	
[C$_6$(mim)$_2$][Tf$_2$N]$_2$	808.66	> −14, < −4		1.52	362 cP	I	M	
[C$_6$(mim)$_2$][BF$_4$]$_2$	421.98	92				M	M	
[C$_6$(mim)$_2$][PF$_6$]$_2$	538.30	136				I	M	
[C$_9$(mim)$_2$][Br]$_2$	450.26	6		1.41	1477 cP	M	I	
[C$_9$(mim)$_2$][Tf$_2$N]$_2$	850.74	−14		1.47	443 cP	I	M	
[C$_9$(mim)$_2$][BF$_4$]$_2$	464.06	−4		1.3		M	M	
[C$_9$(mim)$_2$][PF$_6$]$_2$	580.38	88				I	M	
[C$_{12}$(mim)$_2$][Br]$_2$	492.34	−17		1.27	2008 cP	M	I	
[C$_{12}$(mim)$_2$][Tf$_2$N]$_2$	892.82	−26		1.40	606 cP	I	M	
[C$_{12}$(mim)$_2$][BF$_4$]$_2$	506.14	−19		1.26		PM	M	
[C$_{12}$(mim)$_2$][PF$_6$]$_2$	622.46	9		1.36		I	M	
[C$_9$(bim)$_2$][Br]$_2$	534.42	>0, <23		1.27	>2500 cP	M	I	
[C$_9$(bim)$_2$][Tf$_2$N]$_2$	934.90	>−42, <−8		1.35	550 cP	I	M	
[C$_9$(bim)$_2$][BF$_4$]$_2$	548.22	>−42, <−8		1.20		PM	M	
[C$_9$(bim)$_2$][PF$_6$]$_2$	664.54	>0, <23		1.30		I	M	
[C$_3$(m$_2$im)$_2$][Br]$_2$	394.15	298				M	I	
[C$_3$(m$_2$im)$_2$][Tf$_2$N]$_2$	794.63	91				I	M	
[C$_3$(m$_2$im)$_2$][PF$_6$]$_2$	524.27	264				I		
[C$_9$(m$_2$im)$_2$][Br]$_2$	478.31	174				M	I	
[C$_9$(m$_2$im)$_2$][Tf$_2$N]$_2$	878.79	−42		1.47	687 cP	I	M	
[C$_9$(m$_2$im)$_2$][BF$_4$]$_2$	492.11	>0, <23		1.31		M	M	
[C$_9$(m$_2$im)$_2$][PF$_6$]$_2$	608.43	130				I	M	
[C$_{12}$(benzim)$_2$][Br]$_2$	644.53	151				I	I	
[C$_{12}$(benzim)$_2$][NTf$_2$]$_2$	1045.01	>−8, <0		1.37		I	M	
[C$_{12}$(benzim)$_2$][PF$_6$]$_2$	774.65	−15		1.27		I	ACN	
[C$_3$(mpy)$_2$][Br]$_2$	372.18	51				M	I	
[C$_3$(mpy)$_2$][Tf$_2$N]$_2$	772.67	206				I	M	
[C$_3$(mpy)$_2$][PF$_6$]$_2$	502.30	359				I	M	
[C$_9$(mpy)$_2$][Br]$_2$	456.34	257				M	I	
[C$_9$(mpy)$_2$][Tf$_2$N]$_2$	856.83	>−8, <0		1.41	502 cP	I	M	
[C$_9$(mpy)$_2$][PF$_6$]$_2$	586.46	223				I	M	
[C$_9$(bpy)$_2$][Br]$_2$	540.50	216				M	I	
[C$_9$(bpy)$_2$][Tf$_2$N]$_2$	940.98	84				I	M	
[C$_9$(bpy)$_2$][PF$_6$]$_2$	670.62	249				I	M	
[C(mim)$_2$][I]$_2$	431	>260				M	I	
[C(mim)$_2$][Tf$_2$N]$_2$		90 ~ 94				I	M	
[C$_4$(mim)$_2$][Cl]$_2$	291.97	145 ~ 150				M	I	
[C$_4$(mim)$_2$][Tf$_2$N]$_2$		54 ~ 56				I	M	

Table 2 (Continued) Physiochemical and electrochemical properties of dicationic ionic liquids[33-43, 76-78].

Ionic liquid	M_{w} (g·mol^{-1})	MP(℃)	T_{d} (℃)	Density (g·cm^{-3})	Viscosity	Miscibilitya		ECW (V)
						water	ACN	
Physicochemical Properties of Symmetrical Imidazolium and Pyrrolidinium DILs								
[C$_8$(mim)$_2$][Tf$_2$N]$_2$		25				I	M	
[C$_{10}$(mim)$_2$][Cl]$_2$		25				M	I	
[C$_{10}$(mim)$_2$][Tf$_2$N]$_2$		25				I	M	
[C$_{12}$(mim)$_2$][Cl]$_2$		35 ~ 40				M	I	
[C$_4$(mim)$_2$][Br]$_2$		152.5	297			M	I	
[C$_5$(mim)$_2$][Br]$_2$		137.8	282			M	I	
[C$_3$(bim)$_2$][Br]$_2$		96.2	280			M	I	
[C$_4$(bim)$_2$][Br]$_2$			275			M	I	
[C$_5$(bim)$_2$][Br]$_2$			280			M	I	
[C$_6$(bim)$_2$][Br]$_2$		167.9	279			M	I	
[C$_3$(him)$_2$][Br]$_2$		122.6	280			M	I	
[C$_4$(him)$_2$][Br]$_2$			277			M	I	
[C$_5$(him)$_2$][Br]$_2$			284			M	I	
[C$_6$(him)$_2$][Br]$_2$			279			M	I	
[C$_5$(mim)$_2$][Tf$_2$N]$_2$	794.2	−61	365.2	1.57	251 cSt	I	M	
[C$_5$(hyeim)$_2$][Tf$_2$N]$_2$	854.2	−65	257.4	1.58	241 cSt	I	M	
[C$_5$(bim)$_2$][Tf$_2$N]$_2$	878.3	−62	375.8	1.44	355 cSt	I	M	
[C$_5$(benzim)$_2$][Tf$_2$N]$_2$	946.3	−34.5	291.1	1.55	1209 cSt	I	M	
[C$_5$(tma)$_2$][Tf$_2$N]$_2$	743.2	86 ~ 88	363.7	1.33		I	M	
[C$_6$O$_2$(bim)$_2$][TFSI]$_2$			212	1.40		I	M	5
[C$_2$(mim)$_2$][NTf$_2$]$_2$				1.78		I	M	4.11
[C$_2$(mim)$_2$][PF$_6$]$_2$				1.56		I	M	4.11
[C$_2$(mim)$_2$][BF$_4$]$_2$				1.52		M	M	4.11
[C$_6$O$_2$(mpy)$_2$][TFSI]$_2$			381					6
[C$_8$O$_2$(mpy)$_2$][TFSI]$_2$			366					6
[C$_6$O$_2$(mpip)$_2$][TFSI]$_2$			375					6
[C$_8$O$_2$(mpip)$_2$][TFSI]$_2$			369					6
Physicochemical Properties of Aliphatic Tetraalkylammonium DILs								
[C$_2$(N$_{888}$)$_2$][Br]$_2$	390.24		221.83			M	M	
[C$_3$(N$_{888}$)$_2$][Br]$_2$	404.27	84.97	219			M	M	
[C$_4$(N$_{888}$)$_2$][Br]$_2$	418.29		207			M	M	
[C$_2$(N$_{222}$)$_2$][Br]$_2$	895.20	250.28	266.91			I	M	
[C$_3$(N$_{222}$)$_2$][Br]$_2$	909.22	219.76	266.37			I	M	
[C$_4$(N$_{222}$)$_2$][Br]$_2$	923.25	213.75	249.63			I	M	
[C$_2$(N$_{112}$)$_2$][Tf$_2$N]$_2$	734.62	187	355			I	M	
[C$_2$(N$_{114}$)$_2$][Tf$_2$N]$_2$	790.73	125	342			I	M	
[C$_2$(N$_{116}$)$_2$][Tf$_2$N]$_2$	846.84	84	373			I	M	
[C$_2$(N$_{118}$)$_2$][Tf$_2$N]$_2$	902.94	80	382			I	M	
[C$_3$(N$_{112}$)$_2$][Tf$_2$N]$_2$	748.65	178	377			I	M	
[C$_3$(N$_{113}$)$_2$][Tf$_2$N]$_2$	776.70	124	362			I	M	
[C$_3$(N$_{114}$)$_2$][Tf$_2$N]$_2$	804.76	61	364			I	M	
[C$_3$(N$_{115}$)$_2$][Tf$_2$N]$_2$	832.81	51	363			I	M	
[C$_3$(N$_{116}$)$_2$][Tf$_2$N]$_2$	860.86	64	378			I	M	

Table 2 (Continued) Physiochemical and electrochemical properties of dicationic ionic liquids[33-43, 76-78].

Ionic liquid	M_W (g·mol⁻¹)	MP(ºC)	T_d (ºC)	Density (g·cm⁻³)	Viscosity	Miscibility a		ECW (V)
						water	ACN	
Physicochemical Properties of Symmetrical Imidazolium and Pyrrolidinium DILs								
$[C_3(N_{117})_2][Tf_2N]_2$	888.92	47	389			I	M	
$[C_3(N_{118})_2][Tf_2N]_2$	916.97	47	357			I	M	
$[C_6(N_{112})_2][Tf_2N]_2$	790.73	45	413			I	M	
$[C_6(N_{114})_2][Tf_2N]_2$	846.84	86	401			I	M	
$[C_6(N_{116})_2][Tf_2N]_2$	902.94	51	409			I	M	
$[C_6(N_{118})_2][Tf_2N]_2$	959.05		409	1.17		I	M	
$[C_9(N_{222})_2][Tf_2N]_2$	889.92		410	1.25		I	M	
$[C_{12}(N_{222})_2][Tf_2N]$	930.99	< −60	414	1.31		I	M	
Physicochemical Properties of Asymmetrical DILs								
$[C(mtim)(mim)][Tf_2N]_2$		95	371	1.76		PM	M	
$[C(etim)(eim)][Tf_2N]_2$		52	360	1.71		M	M	
$[C(btim)(bim)][Tf_2N]_2$		−45	334	1.64		M	M	
$[C(tfbtim)(tfbim)][Tf_2N]_2$		65	323	1.76		M	M	
$[C(etim)(mim)][Tf_2N]_2$		65	348	1.73		PM	M	
$[C(btim)(mim)][Tf_2N]_2$		−32	319	1.64		M	M	
$[C(btim)(mim)][PF_6]_2$		150	282	1.66		PM	M	
$[C(tfbtim)(mim)][Tf_2N]_2$		72	319	1.75		M	M	
$[C(mtim)(bim)][Tf_2N]_2$		−37	330	1.69		M	M	
$[C(etim)(bim)][Tf_2N]_2$		−41	348	1.67		M	M	
$[C(tfbtim)(bim)][Tf_2N]_2$		−21	335	1.68		M	M	
$[C_5(tma)(mim)][Tf_2N]_2$	771.2	−51.5	301.5	1.54	357 cSt	I		
$[C_5(tma)(hyeim)][Tf_2N]_2$	801.2	−54.2	132.9	1.54	398 cSt	I	M	
$[C_5(tma)(bim)][Tf_2N]_2$	813.2	−53	389	1.47	527 cSt	I	M	
$[C_5(tma)(benzim)][Tf_2N]_2$	847.3	−36.2	328	1.50	1217 cSt	I	M	
$[C_5(tma)(bpy)][Tf_2N]_2$	816.3	30 ~ 32	356.8	1.46		I	M	
$[C_5(bpy)_2][Tf_2N]_2$	884.4	36 ~ 38	309.5	1.47		I	M	
$[C_5(tma)(mim)][Br]_2$	371.1	115 ~ 116	90.5	1.37		M	I	
$[C_5(tma)(mim)][PF_6]_2$	501.3	86 ~ 88	312.4	1.57		I	I	
$[C_5(tma)(mim)][BF_4]_2$	385.0	>50, <80	336.9			M	I	
$[C_5(tma)(mim)][TfO]_2$	509.5	153 ~ 156	315.9	1.50		M	I	
$[MIC_2N_{111}][TFSI]_2$	729.64	133	360					4 ~ 5
$[MIC_5N_{111}][TFSI]_2$	771.64		420	1.47				4 ~ 5
Physicochemical Properties of Heteroanionic DILs								
$[C_3(Py)(mim)][PF_6][Br]$		150 ~ 151	252			M	I	
$[C_3(Py)(tea)][PF_6][Br]$		180 ~ 181	244			M	I	
$[C_3(Py)(mim)][Tf_2N][Br]$		34 ~ 35	246			M	I	
$[C_3(Py)(tem)][Tf_2N][Br]$		76 ~ 77	240			M	I	
$[C_3(Py)(mpy)][Tf_2N][Br]$		92 ~ 93	249			M	I	
$[C_4(mim)_2][Br]_2$	435.96	167	297			M	M	
$[C_4(mim)_2][AOT]_2$	1118.72	68			7.176 Pa·s	I	M	
$[C_4(mim)_2][FeCl_3Br]_2$	760.4	52			0.2 Pa·s	M	M	
Physicochemical Properties of Dianionic DILs								
$[Hmim]_2[B_{12}Cl_{12}]$		153		1.686		I	M	

Table 2 (Continued) Physiochemical and electrochemical properties of dicationic ionic liquids[33-43, 76-78].

Ionic liquid	M_W (g·mol^{-1})	MP (°C)	T_d (°C)	Density (g·cm^{-3})	Viscosity	Miscibility^a water	Miscibility^a ACN	ECW (V)
\[C$_2$mim]$_2$[B$_{12}$Cl$_{12}$]		265	480	1.614		I	M	
\[C$_3$mim]$_2$[B$_{12}$Cl$_{12}$]		269		1.596		I	M	
\[C$_4$mim]$_2$[B$_{12}$Cl$_{12}$]		131		1.553		I	M	
\[C$_8$mim]$_2$[B$_{12}$Cl$_{12}$]		127		1.387		I	M	
\[C$_{10}$mim]$_2$[B$_{12}$Cl$_{12}$]		174		1.428		I	M	
\[C$_{16}$mim]$_2$[B$_{12}$Cl$_{12}$]		105				I	M	
\[Bnmim]$_2$[B$_{12}$Cl$_{12}$]		256		1.761		I	M	
\[C$_4$C$_1$mim]$_2$[B$_{12}$Cl$_{12}$]		236		1.517		I	M	
\[HEmim]$_2$[B$_{12}$Cl$_{12}$]		275	412	1.671		I	M	
\[N$_{2224}$]$_2$[B$_{12}$Cl$_{12}$]		> 300	444	1.457		I	M	
\[N$_{2226}$]$_2$[B$_{12}$Cl$_{12}$]		221		1.658		I	M	
\[N$_{11116}$]$_2$[B$_{12}$Cl$_{12}$]		104	158	1.216		I	M	
\[N$_{222}$HE]$_2$[B$_{12}$Cl$_{12}$]		295	390	1.563		I	M	
\[PyC$_4$]$_2$[B$_{12}$Cl$_{12}$]		222	398	1.683		I	M	
\[Pppp$_2$]$_2$[B$_{12}$Cl$_{12}$]		293	494	1.656		I	M	
\[C$_4$(mim)$_2$][C$_0$(CO$_2$)$_2$]	308.33	−7.33	230			M	I	
\[C$_4$(mim)$_2$][C$_1$(CO$_2$)$_2$]	322.3596	−0.78	207	1.24		M	I	
\[C$_4$(mim)$_2$][C$_2$(CO$_2$)$_2$]	336.3862	−29.35	235			M	I	
\[C$_4$(mim)$_2$][C$_3$(CO$_2$)$_2$]	350.4127	2.47	249			M	I	
\[C$_4$(mim)$_2$][C$_4$(CO$_2$)$_2$]	364.4393	−27.4	231			M	I	
\[C$_4$(mim)$_2$][C$_5$(CO$_2$)$_2$]	378.4659	−13.34	244	1.15		M	I	
\[C$_6$(mim)$_2$][C$_0$(CO$_2$)$_2$]	336.3862	−29.45	228			M	I	
\[C$_6$(mim)$_2$][C$_1$(CO$_2$)$_2$]	350.4127	−9.36	235	1.20		M	I	
\[C$_6$(mim)$_2$][C$_2$(CO$_2$)$_2$]	364.4393	−1.02	235			M	I	
\[C$_6$(mim)$_2$][C$_3$(CO$_2$)$_2$]	378.4659	−10.78	243			M	I	
\[C$_6$(mim)$_2$][C$_4$(CO$_2$)$_2$]	392.4925	−7.06	238			M	I	
\[C$_6$(mim)$_2$][C$_5$(CO$_2$)$_2$]	406.5191	−18.19	245	1.12		M	I	
\[C$_8$(mim)$_2$][C$_0$(CO$_2$)$_2$]	364.4393	−34	226			M	I	
\[C$_8$(mim)$_2$][C$_1$(CO$_2$)$_2$]	378.4659	−8.48	218			M	I	
\[C$_8$(mim)$_2$][C$_2$(CO$_2$)$_2$]	392.4925	−7.73	234			M	I	
\[C$_8$(mim)$_2$][C$_3$(CO$_2$)$_2$]	406.5191	−31.36	239			M	I	
\[C$_8$(mim)$_2$][C$_4$(CO$_2$)$_2$]	420.5456	−5.74	240			M	I	
\[C$_8$(mim)$_2$][C$_5$(CO$_2$)$_2$]	434.5722	−14.45	238			M	I	
\[C$_{10}$(mim)$_2$][C$_0$(CO$_2$)$_2$]	392.4925	−12.12	223			M	I	
\[C$_{10}$(mim)$_2$][C$_1$(CO$_2$)$_2$]	406.5191	−11.94	218			M	I	
\[C$_{10}$(mim)$_2$][C$_2$(CO$_2$)$_2$]	420.545	3.23	236			M	I	
\[C$_{10}$(mim)$_2$][C$_3$(CO$_2$)$_2$]	434.5722		239			M	I	
\[C$_{10}$(mim)$_2$][C$_4$(CO$_2$)$_2$]	448.5988	−1.65	237			M	I	
\[C$_{10}$(mim)$_2$][C$_5$(CO$_2$)$_2$]	462.6254	0.7	232			M	I	

^{a} Legend: I, immiscible; M, miscible, PM, Partly miscible.

Table 3 Physiochemical and electrochemical properties of dicationic ionic liquids[33-43, 76-78].

Ionic liquid	M_W (g·mol⁻¹)	MP (°C)	T_d (°C)	Density (g·cm⁻³)	Viscosity	Miscibilitya water	ACN	ECW (V)
Physiochemical Properties of TTILs								
[Me₃Benz(bmim)₃][Tf₂N]₃	1372.3	66~69	300	1.55		I	M	
[Me₃Benz(mmim)₃][Tf₂N]₃	1246	82~85	338	1.69		I	M	
[Benz(bmim)₃][Tf₂N]₃	1330.2	−24.6	344	1.53	2320 (cSt)	I	M	
[Benz(mmim)₃][Tf₂N]₃	1203.9	−38.6	364	1.56	1280 (cSt)	I	M	
[Benz(benzmim)₃][Tf₂N]₃	1432.2	−87.4	262	1.55	20000~25000(cSt)	I	M	
[Benz(bmpy)₃][Tf₂N]₃	1339.3	62~64	344	1.44		I	M	
[N(beim)₃][Tf₂N]₃	1311.2	−47.5	308	1.41	1580 (cSt)	I	M	
[N(meim)₃][Tf₂N]₃	1184.9	36~37	338	1.56		I	M	
[N(bepy)₃][Tf₂N]₃	1320.3	57~58	297	1.47		I	M	
[N(CH₂CH₂OHeim)₃][Tf₂N]₃	1275	−38.5	344	1.64	7980 (cSt)	I	M	
[Me₃Benz(bmim)₃][PF₆]₃	924.6	141~143	246	1.49		I	M	
[Me₃Benz(bmim)₃][TFO]₃	937	63~65	316	1.47		M	M	
[Me₃Benz(bmim)₃][BF₄]₃	750.1	130~133	302	1.41		M	M	
[N(beim)₃][PF₆]₃	905.6	195~197	309	1.33		I	M	
[N(beim)₃][TFO]₃	917.9	64.2	253	1.33		M	M	
[N(beim)₃][BF₄]₃	731.1	101~104	274	1.21		M	M	
[C₆O₃(mim)₃][Tf₂N]₃			300			I	M	4
[C₆O₃(dmapy)₃][Tf₂N]₃			340			I	M	5
Physiochemical Properties of LTILs								
[C₁₀(mim)₃][Tf₂N]₃	1352.25	−53.58	334	1.65	1800 (cSt)	I	M	
[C₁₀(mim)₃][Tf₂N]₃	1435.29	−53.17	350	1.54	2400 (cSt)	I	M	
[C₁₀(benzim)₃][Tf₂N]₃	1504.44	−36.61	320	1.36	4200 (cSt)	I	M	
[C₁₀(bim)₃][BF₄]₃	856.55	−18.32	191	1.33		M	M	
[C₁₀(bim)₃][TFO]₃	1043.18	−42.63	290	1.28		M	M	
[C₆(mim)₃][Tf₂N]₃	1240.03	−57.85	320	1.57	372 (cSt)	I	M	
[C₆(bim)₃][Tf₂N]₃	1324.19	−51.54	330	1.41	429 (cSt)	I	M	
[C₆(benzim)₃][Tf₂N]₃	1391.14	−36.83	340	1.43	840 (cSt)	I	M	
[C₃(mim)₃][Tf₂N]₃	1155.88	−24.54	290	1.54	1200 (cSt)	I	M	
[C₃(bim)₃][Tf₂N]₃	1240.04	−44.13	310	1.48	600 (cSt)	I	M	
[C₃(benzim)₃][Tf₂N]₃	1308.07	−27.26	300	1.41	4080 (cSt)	I	M	
[C₂(Morp)(im)(Morp)][(2MsO)₂(Cl)]	523.06		298.3	1.283	444.29±16.77(cP)	M	M	
[C₂(2MeAP)(im)(2MeAP)][(2MsO)₂(Cl)]	593.16		280.6	1.274	10807.88±510.33(cP)	PM	M	
[C₂(Morp)(im)(Morp)][(2PhsO)₂(Cl)]	647.20		331.1	1.274	5368.37±6.21(cP)	M	M	
[C₂(MePip)(im)(MePip)][(2MsO)(Cl)(2PhsO)]	673.29		351.2	1.215	6421.29±417.93 (cP)	M	M	
[C₂(2MeAP)(im)(2MeAP)][(2PhsO)₂(Cl)]	717.30		342.6	1.301	13922.29±611.31 (cP)	I	M	
[C₂(mim)₃][(PhsO)(Cl)(2PhsO)]	637.17		338.5	1.304	2839.03±5.66(cP)	M	M	
[C₂(MorP)(im)(MorP)][(2PhsO)₂(OAc)]	670.79		342.8	1.272	2249±7.51(cP)	I	M	

Table 3 (Continued) Physiochemical and electrochemical Properties of Tricationic Ionic Liquids[44-46].

Physiochemical Properties of TTILs								
Ionic liquid	M_w (g·mol^{-1})	MP (°C)	T_d (°C)	Density (g·cm^{-3})	Viscosity	Miscibility[a]		ECW (V)
						water	ACN	
[C$_2$(MePip)(im)(MePip)][(2PhsO)$_2$(OAc)]	696.88		345.6	1.186	3632.37± 29.93 (cP)	I	M	
[C$_2$(2MeAP)(im)(2MeAP)] [(2PhsO)$_2$(OAc)]	740.89		338.0	1.277	4049.49± 127(cP)	PM	M	
[C$_2$(mim)$_3$][(2PhsO)$_2$(OAc)]	660.76		347.4	1.278	3687.69± 23.4(cP)	I	M	
[C$_2$(MorP)(im)(MorP)] [(2PhsO)$_2$(CF$_3$OAc)]	724.76		352.5	1.278	2859.14± 7.44(cP)	I	M	
[C$_2$(MePip)(im)(MePip)] [(2PhsO)$_2$(CF$_3$OAc)]	750.85		350.2	1.241	4948.51± 13.49(cP)	I	M	
[C$_2$(2MeAP)(im)(2MeAP)] [(2PhsO)$_2$(CF$_3$OAc)]	794.86		333.8	1.292	4321.17± 12.85(cP)	I	M	
[C$_2$(mim)$_3$][(2PhsO)$_2$(CF$_3$OAc)]	714.73		307.7	1.297	1360.17± 10.37(cP)	I	M	
[C$_2$(MorP)(im)(MorP)][2PhsO]$_3$	782.94		337.9	1.279	3888.43± 37.06(cP)	I	M	
[C$_2$(2MePip)(im)(2MePip)][2PhsO]$_3$	853.04			1.269	1475.29± 122.27 (cP)	M	M	
[C$_2$(mim)$_3$][2PhsO]$_3$	772.91			1.172	11124.29± 144.35 (cP)	I	M	

[a] Legend: I, immiscible; M, miscible, PM, Partly miscible.

than those of the imidazolium-based OILs[76-78]. Significantly, OILs owing the ether-based spacers even have a very wide ECW (up to 6 V vs. Li/Li$^+$), which surpasses the ECWs of MILs and PILs[52]. In conclusion, OILs are suitable electrolytes for supercapacitors and LIBs.

2.3 Computational Studies of Nano-Organizations of OILs

Compared with the configuration of the isolated cation or anion, the ones of the ion pairs (the neutral ion pair is comprised of a dominant multication and the corresponding number of anions) of OILs are more complex. Hence, figuring out the nano-organizations of the ion pairs and the interionic interactions between ions is quite necessary for OILs, which can further help to understand the relations between the microstructures and physical chemistry properties of OILs.

2.3.1 Nano-Organization of DILs

The geometric and electronic structures of DILs

are investigated by the DFT calculations to account for the variation tendency of some physical properties. The findings on [C$_3$(mim)$_2$][Br]$_2$ and the boron-based DIL [C$_5$(mim)$_2$][BMB]$_2$ showed that the most stable ion pair is found as the two imidazolium rings are tightest, which is contrary to the isolated dication. This is caused by the fact that the two anions in DILs surround the two rings symmetrically and by the addition of the dications-anions interactions[81, 82]. The gained stable structures of DILs mainly are determined by the dications-anions electrostatic attraction and hydrogen bond interactions between anions and the strong acidic hydrogen atoms of the imidazolium rings. Owing to an extra positively charged ring, the interactions in DILs are greater than those in the corresponding MILs. Consequently, the melting point, viscosity, and thermal stability of DILs are greater than those of corresponding MILs (Table 2). Besides, the geometrical characteristics of DILs are also significantly affected by their anionic nature. The DFT

calculation for $[C_3(mim)_2][Cl]_2$ and $[C_3(mim)_2][Br]_2$ demonstrated that the most stable ion pair has two parallel imidazolium rings and anions orienting toward the rings to form hydrogen bonds[62]. However, there are no hydrogen bonds to be detected in $[C_3(mim)_2][I]_2$, since I^- ions are located almost perpendicular to the rings[62].

Additionally, MD simulations can give molecular insight into the structural characteristics. For example, the diverse radial distribution functions (RDFs) between components in DILs with the dications $[C_n(mim)_2]^{2+}$ (n = 3, 6, 9, 12) and anions such as $[Tf_2N^-]$, $[BF_4^-]$, $[PF_6^-]$, $[Br^-]$ are computed to reveal the correlations of different components and the local structures of DILs (Figure 4(A))[69, 79, 83]. Regardless of the linker length of dication, the RDFs between an-

ions and dications declare that all anions homogeneously dwell close to the imidazolium rings and incline toward the hydrogen atoms of the rings; meanwhile, the anion-rings distance increases with the increasing anion volume. As shown in Figure 4(B), the spatial distribution function (SDF), a qualitative supplement for RDFs, also delivers a visualized 3D image that anions are mainly located around the charged rings of dications, and uniformly distributed around three hydrogens in rings. In addition, the SDFs and RDFs of $[PF_6^-]$ around $[C_9(mim)_2]^{2+}$ show that the anions give priority to binding to the hydrogen atom linked with the carbon between two nitrogen atoms (Figure 4(C)), which is line with the results obtained by DFT methods[61]. Furthermore, it is proved by RDFs that the anions-anions interactions
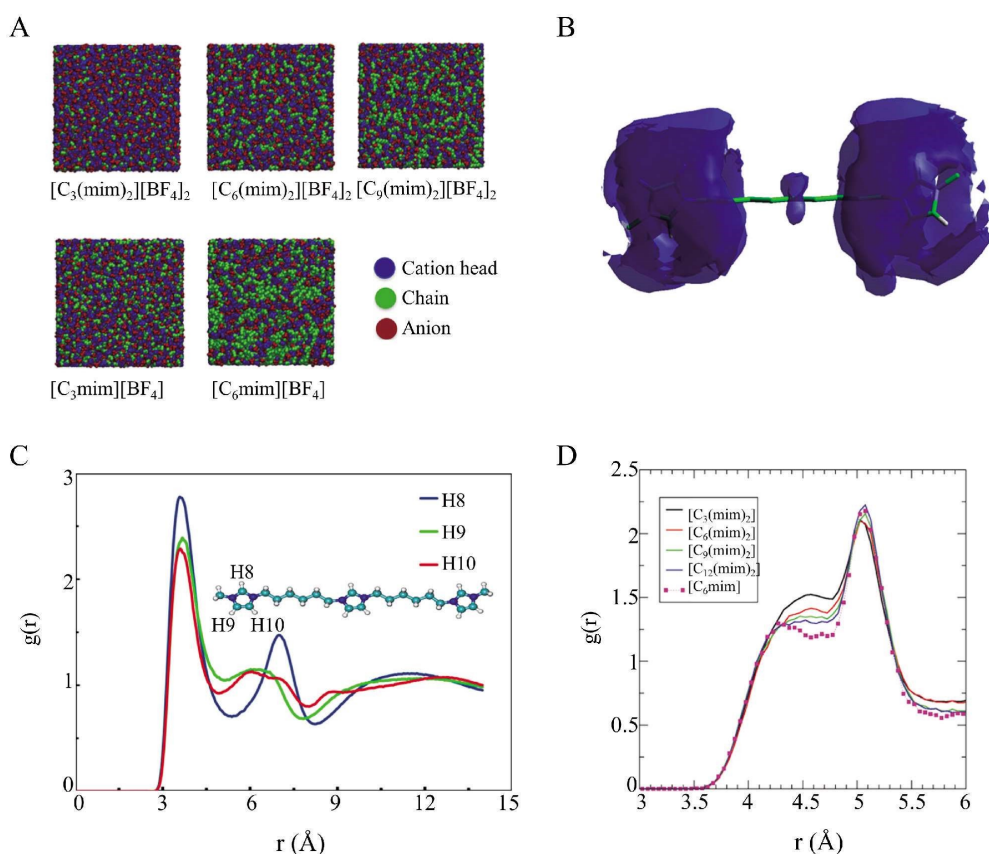
Figure 4 (A) Simulation models of DILs $[C_n(mim)_2][BF4]_2$ (n = 3, 6, 9) and MILs $[C_nmim][BF_4]$. Reproduced with permission of Ref. 83, Copyright 2013, American Chemical Society. (B) SDFs of anions $[PF_6]^-$ around the dication $[C_9(mim)_2]^{2+}$. Reproduced with permission of Ref. 61, Copyright 2012, American Chemical Society. (C) RDFs of $[PF_6]^-$ around three H atoms in dicationic rings. Reproduced with permission of Ref. 61, Copyright 2012, American Chemical Society. (D) C-C RDFs in the anions $[Tf_2N]^-$ of four DILs and a MIL. Reproduced with permission of Ref 69, Copyright 2011, American Chemical Society. (color on line)

are independent of the spacer linker length in dications. The cis conformations of anions are observed, as shown in Figure 4 (D), which origins from that the two charged rings simultaneously provide hydrogen to coordinate with the same anion. As the linker length increases, there is a corresponding shift in how the spacer linkers interact, and the linker seems more stretched. The angle generated by the normal vectors of the two charged rings and the torsional distribution along the linker in $[C_n(mim)_2][Tf_2N]_2$ is computed to further analyze the structure of the two charged rings in the same dication. It should be highlighted that no ring-ring contact or particular orientation is discovered. Moreover, there is no difference between the torsion angle and that in the corresponding MIL[69].

The structure factors and the heterogeneity order parameter (HOP) also serve as essential tools for identifying the overall spatial structures of OILs, and the influence of the spacer linker length, anions nature, and temperature on the heterogeneity. According to the nano-organizations of diimidazolium-based DILs[83, 84], the aggregations of the spacer linkers in dications are dominant in all heterogeneous region blocks. However, the negligible pre-peaks and smaller HOPs of the linkers indicate more modest aggregations and less heterogeneity compared with the MILs, which is ascribed to the fact that the most straight linkers and a few linkers intertwined together in DILs impede the aggregation. These results indicated that the various 3D architectures of bulk DILs are mostly caused by the divergence of the interaction between linkers. Due to the weakened electrostatic repulsion caused by a longer linker, the DILs characterized by a long linker exhibit more aggregation, which is evident by the greater structure factor (Figure 5(A)).

Moreover, the effect of the anionic characteristics on the structures is also explored. Based on the calculated structure factors, it is shown that the aggregation in DILs varies in this order: $[Br^-] > [PF_6^-] > [BF_4^-]$, in line with the inspection in MILs[83]. In addition, the nano-aggregations of the various components in dications and anions are irrelevant to the temperatures, according to the insignificant disparity in HOPs. It is noteworthy that the influence of the side chain length

on the 3D structures of DILs is also unveiled. As shown in Figure 5(B), the MD simulations indicate that the heterogeneity dramatically increases when the side chain lengthens from $[C_5(mim)_2][Tf_2N]_2$ to $[C_5(bim)_2]$ $[Tf_2N]_2$, which is ascribed to the strong correlations between side chains[85]. In contrast to MILs, the uniformity of dicationic charged heads plays a vital role in the structures of DILs. The heterogeneity becomes more obvious by replacing one of the double imidazolium rings with an ammonium group, due to the shorter distance between ammonium-based and imidazolium-based charged heads, as verified by RDFs and SDFs in Figure 5(C)[68].

The microstructural heterogeneity of ILs can lead to dynamical heterogeneity[68, 75, 85]. As illustrated in Figure 5(D), the time correlation functions are applied to estimate the dynamical heterogeneity. Compared with MILs, the correlation function of DILs attenuations more sluggishly, suggesting that ion pairs in DILs are more stable. The structural stability of ion pairs determines the ionic migration rate, hence, the dicationic diffusion is quite sluggish. Moreover, according to the relaxation time, the kinetic heterogeneity of the asymmetrical DIL is larger than that of the diimidazolium-containing DIL, and the kinetic migration of the asymmetrical dications owing to more freedom is faster.

2.3.2 Nano-Organization of TILs

The attentiveness has recently been directed toward the intrastructures of LTILs $[C_n(mim)_3][Tf_2N]_3$ (n = 3, 6, 10)[63, 67]. Similar to the arrangement of DILs, the SDF demonstrated that the majority of anions tightly surround the central rings of the trications, as shown in Figure 6(A-B)[67]. Meanwhile, the trication bends into a helical framework, in which the central ring and two spacer chains form an obtuse angle. This can enhance the ring-anion attractive interaction and weaken the coions-coions repulsion. As shown in Figure 6(C), the spacer linkers between rings have more aggregation with increasing length, in line with DILs. The DFT calculations further reveal that various hydrogen bonds, including the dominant one between anions and hydrogens in rings and the inferior one formed by anions and hydrogens in spacers, are
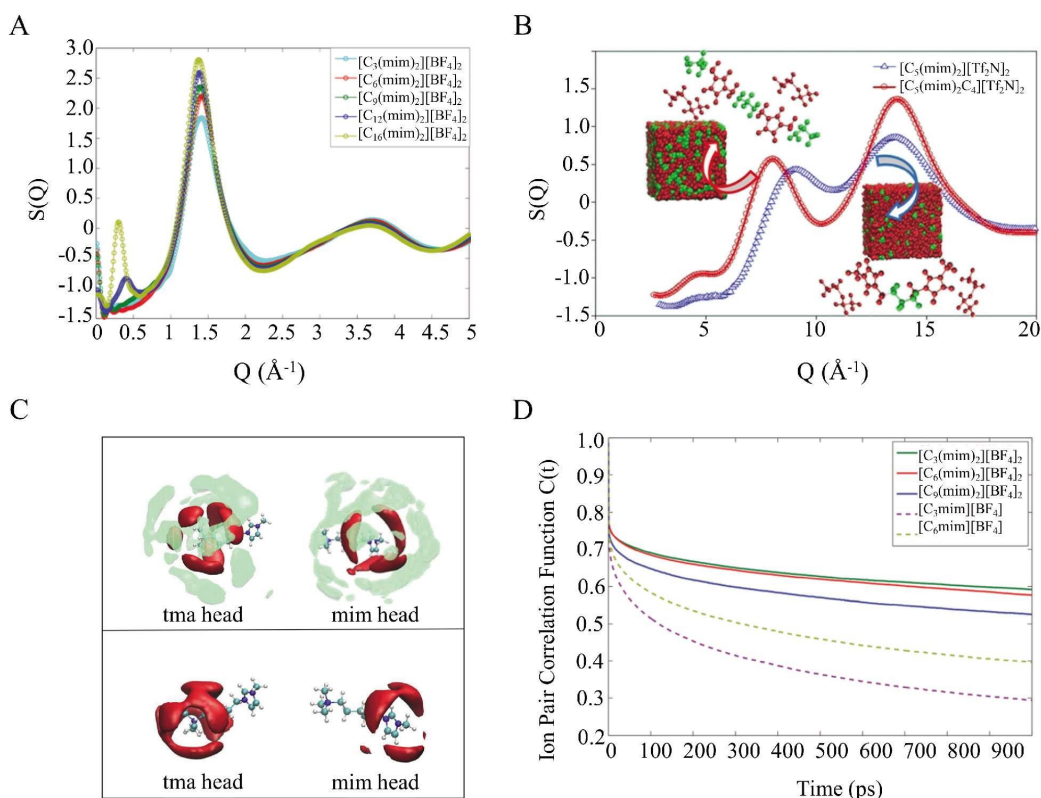
Figure 5 (A) Total static structure factor of $[C_n(mim)_2][BF_4]_2$ (n = 3, 6, 9, 12, 16). Reproduced with permission of Ref. 83, Copyright 2013, American Chemical Society. (B) Total static structure factor of the DILs with the different side chain lengths. Reproduced with permission of Ref. 85, Copyright 2020, American Chemical Society. (C) SDFs of the symmetrical and unsymmetrical DILs. Reproduced with permission of Ref. 68, Copyright 2021, Elsevier. (D) The time correlation functions of the ion pairs in DILs $[C_n(mim)_2]$ $[BF_4]_2$ (n = 3, 6, 12). Reproduced with permission of Ref. 84, Copyright 2014, Royal Society of Chemistry. (color on line)

responsible for the helical frameworks of cations. The order of dominant hydrogen bonds is $[C_{10}(mim)_3]$ $[Tf_2N]_3 > [C_6(mim)_3][Tf_2N]_3 > [C_3(mim)_3][Tf_2N]_3$, which matches exactly with the comparison of viscosity values in Table 3. Whereas, the anions-linkers and linkers-linkers dispersion interactions which hinder the ionic gathering in $[C_3(mim)_3][Tf_2N]_3$ and $[C_{10}(mim)_3]$ $[Tf_2N]_3$, are greater than those in $[C_6(mim)_3][Tf_2N]_3$, leading to the fastest ionic diffusion in $[C_6(mim)_3]$ $[Tf_2N]_3$. As can be seen from Figure 6(D), unlike the heterogeneity characteristics of DILs and MILs, the HOPs of TILs indicate that the tricationic heads hold a greater heterogeneity relative to the constrained spacer linkers.

2.3.3 Impurity Effect on the Nano-Organization of OILs

In addition, in practical applications, OILs can imbibe water from humid surroundings regardless of hydrophilic and hydrophobic characteristics. Hence, many works have been carried out to unveil the structures of the DIL/water mixtures. Notably, dications in [Br⁻]-based DILs spontaneously assemble by interlinking charged rings into hexagons, which is different from the ball-shaped aggregations in MILs/water solutions. Water molecules prioritize interrelations with the anion [Br⁻] regardless of the water content, as revealed by various RDFs among different species, and the first water shell enclosing [Br⁻] gets more congested as the water content rises[86-88]. Moreover, the spacer length between rings plays a crucial role in the intrastructures of the DIL/water mixtures. It is observed that the structures of the DIL/water change from homogeneity to heterogeneity with the elongation of the spacer length. In addition, the coordination
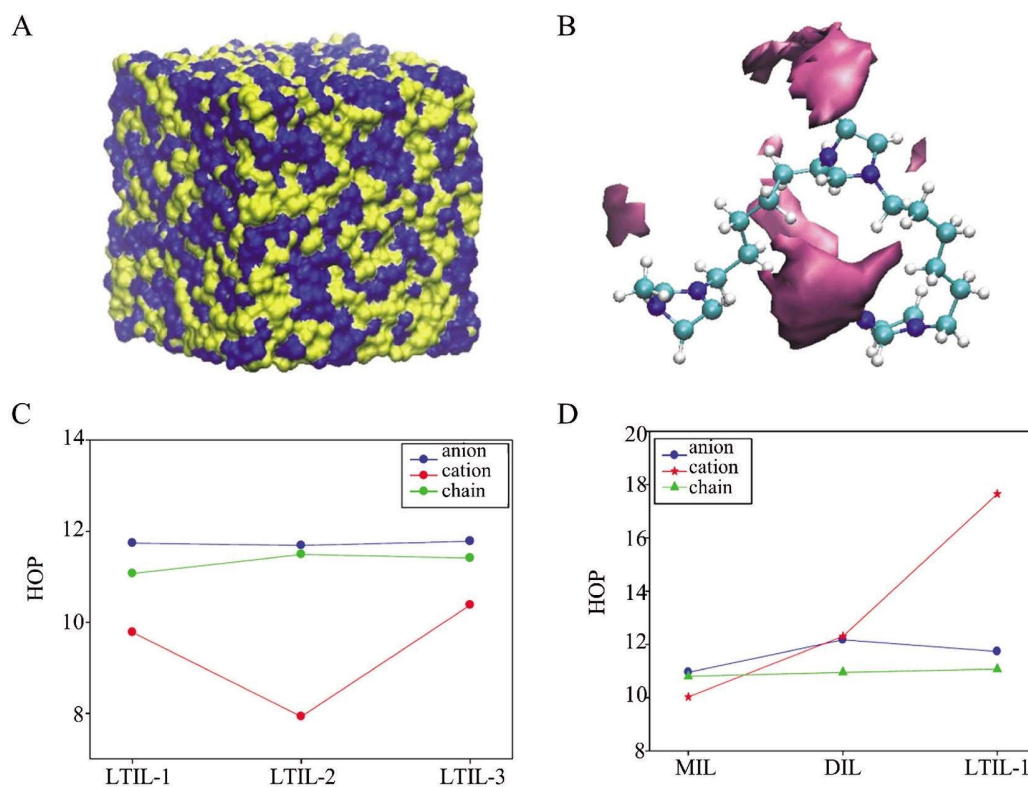
Figure 6 (A) Snapshot of the simulation of [C$_6$(mim)$_3$][Tf$_2$N]$_3$, cations and anions are denoted in yellow and blue, respectively. Reproduced with permission of Ref. 67, Copyright 2017, American Chemical Society. (B) SDFs of the anion around the dication in [C$_6$(mim)$_3$][Tf$_2$N]$_3$. Reproduced with permission of Ref. 67, Copyright 2017, American Chemical Society. (C) HOP of spacer chains, trication rings and anions of LTIL-1 [C$_3$(mim)$_3$][Tf$_2$N]$_3$, LTIL-2 [C$_6$(mim)$_3$][Tf$_2$N]$_3$, and LTIL-3[C$_{10}$(mim)$_3$][Tf$_2$N]$_3$. Reproduced with permission of Ref. 63, Copyright 2018, Elsevier. (D) HOP of different groups in the MIL [C$_3$mim][Tf$_2$N] DIL [C$_3$(mim)$_2$] [Tf$_2$N]$_2$ and LTIL-1 [C$_3$(mim)$_3$][Tf$_2$N]$_3$. Reproduced with permission of Ref. 63, Copyright 2018, Elsevier. (color on line)

number of anions around dications decreases as the linker length extends in the DILs/water mixtures. This is because an anion will contemporaneously interact with two heads in a DIL molecule with a short spacer, however, the long-spacer dication structure, comprised of the two parallel rings and the spacer chain vertical to the rings, impeds the associations between anions and charged heads[89].

3 Application of OILs-Based Electrolytes

3.1 OILs Used in Supercapacitors

Owing to the broad electrochemical window, OILs electrolytes have drawn much attention in supercapacitors storing energy by the charge accumulation in the electrical double layers (EDLs). To figure out the capacitive abilities of OILs electrolytes have to in-

spect the EDLs. Most recently, the EDL properties of OILs at the distinct charged electrodes are revealed by MD simulations, focusing on the interfacial structures and the relationships of the capacitance and electrode voltage.

As is known, the spacer length dramatically influences the physical chemistry properties and intrastructures of DILs. Also, the spacer length may be an important influence factor on the structures and capacitance of EDLs of DILs in supercapacitors. It is proved that the DIL with the shortest spacer exhibits the lowest dications-electrode interaction and strongest dications-anions connection in [C$_n$(mim)$_2$] [BF$_4$]$_2$ (n = 3, 6, 9)/graphene EDLs, leading to the unique two-peaks dication layer near the electrode, which is quite different from the single-peak layers of the cations with the longer spacer length. Moreover, in

contrast to the side chain gradient toward the electrode in [C$_3$mim]$^+$, the spacer linker constrained by two rings gets parallel with the electrode. Furthermore, it can be seen from Figure 7(A) that the *C-V* curve changes from camel to a slight bell shape when the spacer length is extended. This transition can be ascribed to the weak dications-anions attraction and enhanced packing of the charges on the electrode with the extension of the spacer length. Moreover, according to the mean-field theory, the larger capacitive values are observed under positive voltages due to the different counterions volume near the two electrodes[65].

In addition, the dicationic symmetry also plays a vital role in the EDLs properties[90]. For instance, MD simulations illustrate that compared with [C$_6$(tma)(mim)][Tf$_2$N]$_2$, the ionic gathering of the diimidazolium group is denser and closer to the electrode, which is because the imidazolium rings are more parallel to the electrode relative to the ammonium-based ring, as shown in Figure 7(B-C). Whereas, the capacitance of EDLs is insusceptible to the dicationic symmetry within the applied electrode voltages[90].

In terms of the topology of the electrode, the cooperation between the outstanding OIL electrolytes and curved-surface electrodes with enough accessible
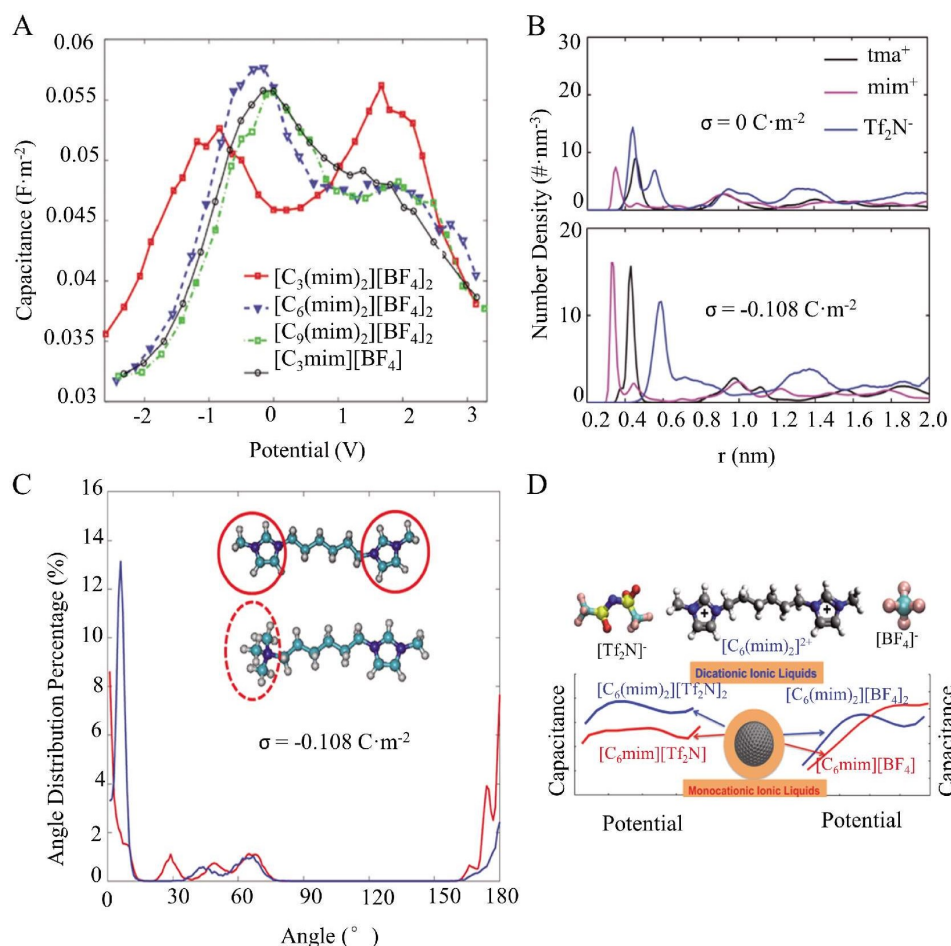
Figure 7 (A) Differential capacitance-voltage curves of the MIL and DILs/planar electrode EDLs. Reproduced with permission of Ref. 56, Copyright 2014, IOP science. (B) Number density profiles of groups in the asymmetrical DIL [C$_6$(tma)(mim)][Tf$_2$N]$_2$ on the uncharged (top) and negatively charged electrodes (bottom). Reproduced with permission of Ref. 90, Copyright 2016, IOP science. (C) The orientation of the spacer chain of the unsymmetrical DIL near the charged surface. Reproduced with permission of Ref. 90, Copyright 2016, IOP science. (D) The capacitance as a function of the OLC electrode potential for MILs and diimidazolium DILs with [Tf$_2$N]$^-$ or [BF$_4$]$^-$. Reproduced with permission of Ref. 57, Copyright 2014, American Chemical Society. (color on line)

surface space is regarded as a valid way to achieve the high performance of supercapacitors. Nevertheless, the aforementioned research above keeps a watchful eye on DILs/planar electrodes EDLs. Feng et al.[57] firstly studied the structures and energy-stored performance of DILs/Onion-like carbon (OLC) electrode EDLs by MD simulations (Figure 7(D)). In comparison with the MIL, more anions in DILs gather on the electrode to neutralize the extra positive charge of dications. Moreover, the direction of spacer linkers and rings in dications changes from parallel to vertical relative to the electrode, which is in line with MIL/OLC but dissimilar to the DIL/planar electrode. Interestingly, the *C-V* curves on the OLC electrode can be defined as neither the bell nor camel type. In addition, the capacitance under negative voltages declines as the spacer length is lengthened, which is ascribed to limited packed dications with a long spacer on the electrode. Delightedly, DIL $C_6(mim)_2][Tf_2N]_2$ exhibits greater capacitance throughout applied voltages, compared with the corresponding MIL.

Recently, we have focused on the LTILs/graphene EDLs with the aid of MD simulations[59]. Specifically, the trications exhibit an inferior packing ability on the negatively charged electrode when compared to MILs and DILs, which mainly stems from a tradeoff between the larger sizes and stronger trication-electrode attractive interaction. However, more anions [Tf_2N^-] of LTILs gather on the positive electrode to balance the tricationic charge. Unlike the parallel cations of MILs and DILs, the two side rings of trications are parallel to the negative electrode, while the ring in the midpoint remains vertical, particularly in the long-spacer LTIL. Moreover, as shown in Figure 8(A), the bell-shaped *C-V* curve in the MIL transforms into the camel shape in LTILs. Such transition is caused by the dense accumulation of charged rings and anions of LTILs on the charged electrodes, which induces a saturation phenomenon at the capacitive peak.

In contrast to MILs electrolytes, the sluggish ion dynamics of OILs hampers their application on supercapacitors. Fortunately, it is observed from MD works

that incorporating proper organic solvents such as acetonitrile (ACN), ethylene carbonate (EC), and propylene carbonate (PC) into OILs can significantly boost ionic mobility and enhance the energy density[91]. Specifically, the migration rates of the cations [$C_6(mim)_2$]$^{2+}$ and anions [Tf_2N]$^-$ in DIL significantly increase with the addition of ACN. The conductivity, thereby, rises to tens of times as large as that of the neat DIL under a certain DIL content, and subsequently, continues to decrease due to the very low ion content in the mixed liquid. Hence, it is intriguing to elucidate the influence of organic solvents on the EDL structure with DIL/organic solvent electrolytes[91]. It was found that, compared to the EDL of the pure DIL, there are fewer counterions nearby the electrode surface due to the packing of organic solvents. The dications-anions connections can be weakened by organic solvents, hence more co-ions are seen to be ejected from the charged electrode, particularly in PC. Additionally, the *C-V* curves still maintain the bell shape, with the capacitive values slightly larger than that of the pure DIL.

For higher-viscosity TILs, as expected, the addition of ACN or carbonate EC induces the same change trend in the dynamic performance with DILs. By comparison in Figure 8(B), although the greater dielectric strength of EC can promote the dissociation of ion pairs and ionic migration, the conductivity of TIL/EC has a modest enhancement relative to that of TIL/ACN regardless of the proportion of the TIL in the mixture as a result of the higher viscosity of EC[80]. The organic solvents ACN and EC are added to the TIL electrolytes to reduce the high viscosity and the obtained $0.55 \text{ mol} \cdot L^{-1}$ [$C_6(mim)_3$](Tf_2N)$_3$/ACN has the biggest conductivity. Therefore, the $0.55 \text{ mol} \cdot L^{-1}$ TIL/ACN is regarded as an outstanding substitute for the neat TILs electrolytes in supercapacitors. Like the role of ACN in the DIL/ACN electrolyte, solvent molecules impede the accumulation of larger-size trications on the negative electrode, as shown in Figure 8(C). For capacitance (Figure 8(D)), the shape of the *C-V* curve is insensitive to the presence of solvents, comparatively speaking, the integral capacitances in TIL/ACN
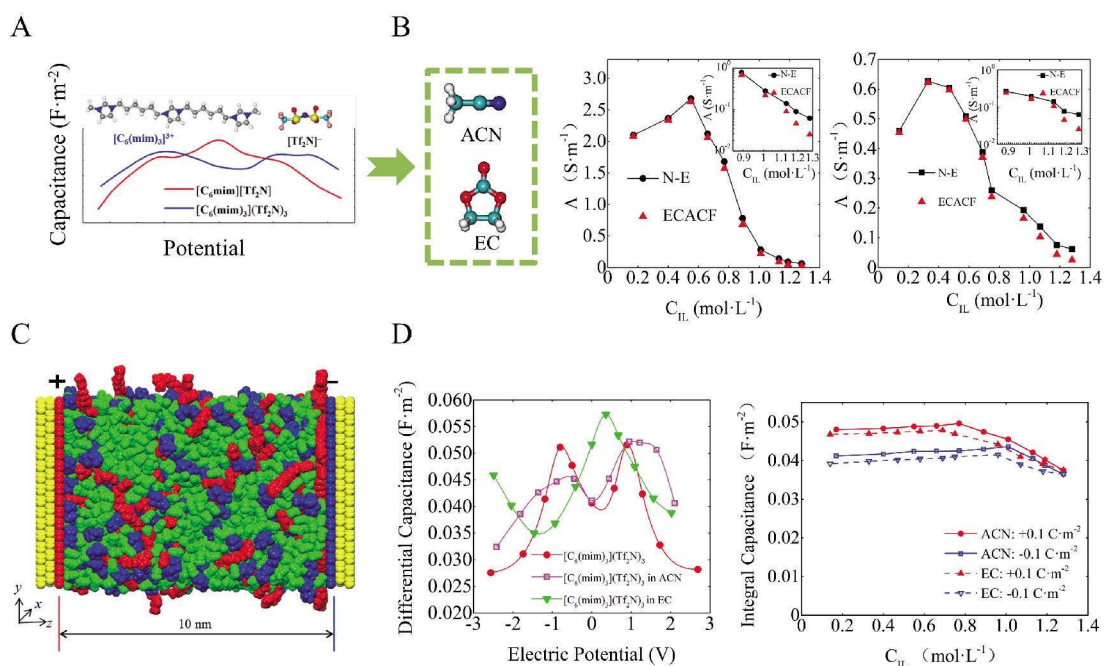
Figure 8 (A) Difference capacitance as a function of the planar electrode potential for the MIL[C_6mim][Tf_2N] and LTILs [C_6(mim)$_3$] [Tf_2N]$_3$. Reproduced with permission of Ref. 59, Copyright 2020, American Chemical Society. (B) Conductivities of the LTIL in ACN (left) and EC (right) as a function of the LTIL concentrations. Reproduced with permission of Ref. 80, Copyright 2021, American Chemical Society. (C) Structures of EDLs comprised LTIL/ACN and TIL/EC electrolytes and planar graphite electrodes. Reproduced with permission of Ref. 80, Copyright 2021, American Chemical Society. (D) Difference capacitance-voltage curves of the pure LTIL and mixed electrolytes (left), and the integral capacitance (right) as a function of the LTIL concentrations in LTIL/ACN and TIL/EC electrolytes. Reproduced with permission of Ref. 80, Copyright 2021, American Chemical Society. (color on line)

and TIL/EC are greater than that in the neat TIL throughout applied TIL concentrations, especially in TIL/ACN, accomplishing both intensive power density and energy-stored capacity[80].

Until recently, there has been little research into the investigation of EDLs of tetracationic ILs. The experiment has verified that the tetracationic IL with four imidazolium heads connected by three ether-based spacers owns a very large operating voltage and excellent capacitive capacity[52]. Stimulated by this, the inherent principles of the tetracationic accumulation on the nanoporous electrode are explored by applying the classical DFT[60]. Unlike the [C_4mim] [Tf_2N]/nanoporous electrode EDL, the large cations and more anions within pores are not detected until the imposed voltages reach a specific level, as depicted in Figure 9(A,B), leading to increased capacitance. Then ionic saturation inside pores appears,

causing the decline of capacitance, resulting in the camel-like *C-V* curves (Figure 9(C)). In comparison with the MIL, the energy density of EDLs is remarkably increased under the high negative voltages but dramatically depletes throughout positive voltages, as shown in Figure 9(D).

3.2 OILs Used in Lithium-Ion Batteries

The traditional mixed organic electrolytes applied in LIBs suffer from low flash points and a narrow liquid temperature range[92]. Owing to the non-burning advantage, better temperature tolerance, and lower vapor pressure, DILs are regarded as candidates for LIBs. Recently, the performance of the LiPF$_6^-$ based LIB with DIL/organic solution including EC and DMC (1:1) has been investigated[76]. As shown in Figure 10(A), the performance of LIBs at high temperature is much improved when compared to that of LIB without DIL. Specifically, the flash point of the elec-
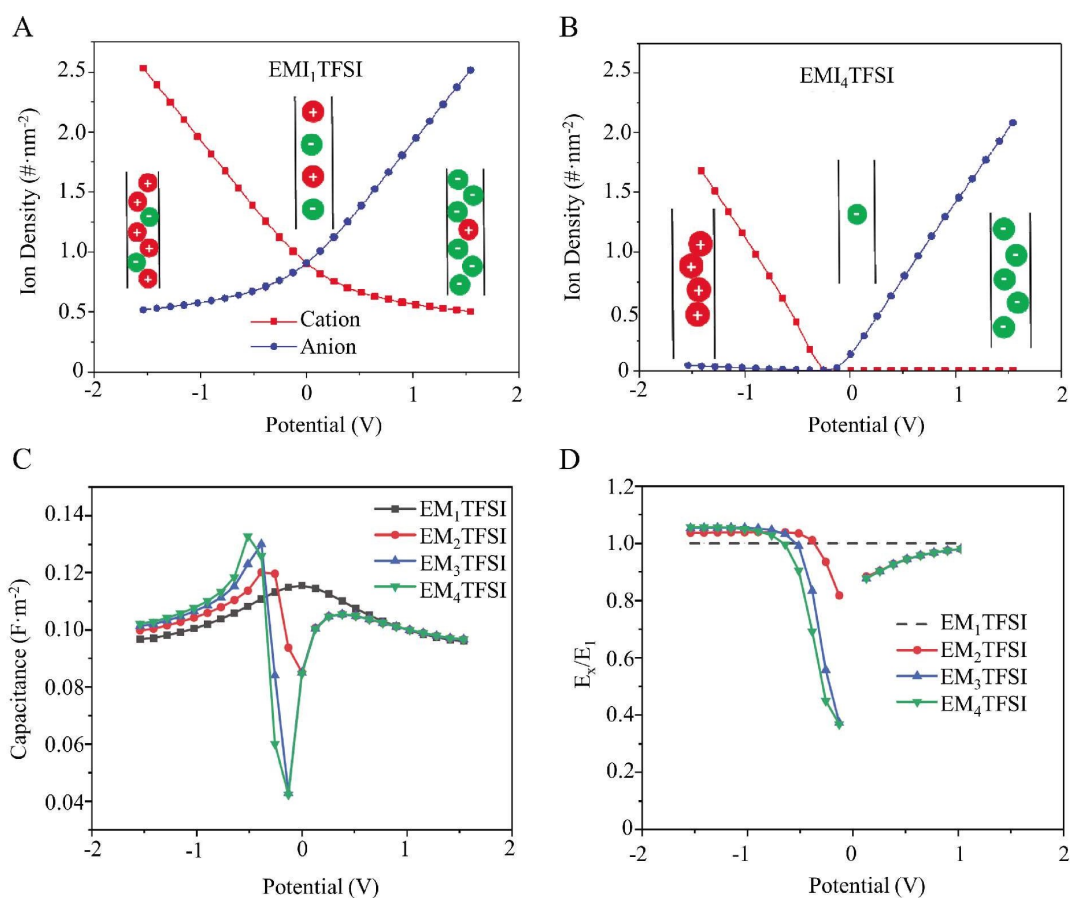
Figure 9 Density distribution of the MIL [C₄mim][Tf₂N] (EM1TFSI) (A) and the imidazolium tetracationic ILs (EM₄TFSI) with the ether-based spacers (B) inside the nanopore. Differential capacitance (C) and the normalized energy density (D) as a function of the electrode potential for MIL [C₄mim][Tf₂N] and multicationic ILs, such as DIL (EM₂TFSI), TIL (EM₃TFSI), and EM₄TFSI. Reproduced with permission of Ref. 60, Copyright 2018, American Chemical Society. (color on line)
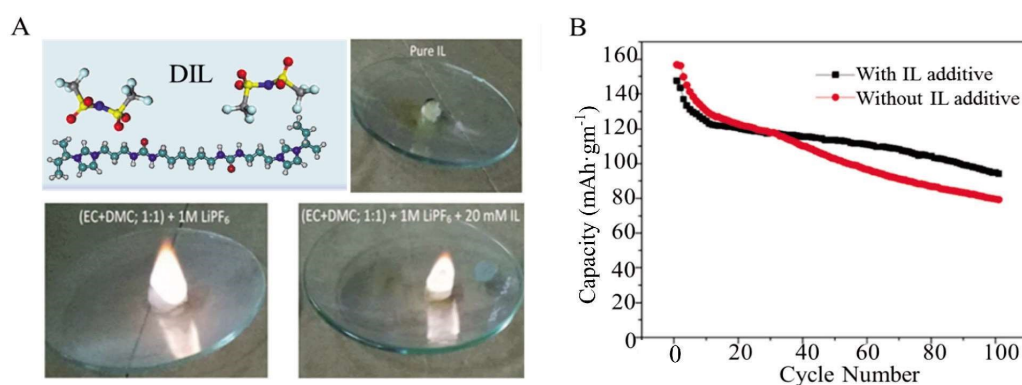

Figure 10 (A) Flammability of the organic electrolytes with and without the DIL. Reproduced with permission of Ref. 76, Copyright 2018, Nature Publishing Group. (B) Cycling stability of LIBs in the electrolytes with and without DIL. Reproduced with permission of Ref. 76, Copyright 2018, Nature Publishing Group. (color on line)

trolyte rises by around 30 °C with the addition of the 0.02 mol·L⁻¹ DIL. Meanwhile, the addition of DIL

preserves the electrochemical window without lowering its electrical conductivity. Consequently, the organic

electrolyte with DIL demonstrated an excellent performance with a long cycling ability and mass discharge capacities (Figure 10(B)).

Interestingly, a widened operating voltage window of the $[C_6(tma)(mim)][Tf_2N]_2$, $[C_6(tea)(mim)][Tf_2N]_2$ or $[C_6(tba)(mim)][Tf_2N]_2$ electrolyte is observed in LIBs, contrast to imidazolium-based MILs[77]. Moreover, the conductivity of the asymmetrical DILs electrolytes is affected by the length of the side chain linking the ammonium group, it is concluded from Figure 11(A,B) that the 1 mol·L^{-1} LITFSI mixed $[C_6(tea)(mim)][Tf_2N]_2$ mixture is the top-class electrolyte among asymmetrical DILs-based LIBs studied, owing the strongest rate ability, energy-storage capacity, and incombustibility. The other components significantly affecting the thermotolerance and elec-

trochemistry characteristics of LIBs are the charged heads of the dications as well as the length and category of the spacers[93]. It is confirmed that the LiTFSI/DILs with the shortened ether-including spacers solutions own larger operating voltage (about 6.0 V in Figure 11(C)) regardless of the category of the charged heads. Furthermore, the pyrrolidinium DIL with the shorter spacer in the LIB presents a quicker Li$^+$ transference rate compared with the longer-spacer DIL with the same heads and piperidinium-dominated DILs, which is supported by the weakest Li$^+$-TFSI-correlation, as shown in Figure 11(D). Considering the category of the spacer, utilizing DILs with the ether groups rather than —CH$_2$— units as electrolytes will heighten the specific capacity of the LIBs.

In summary, in comparison with the corresponding

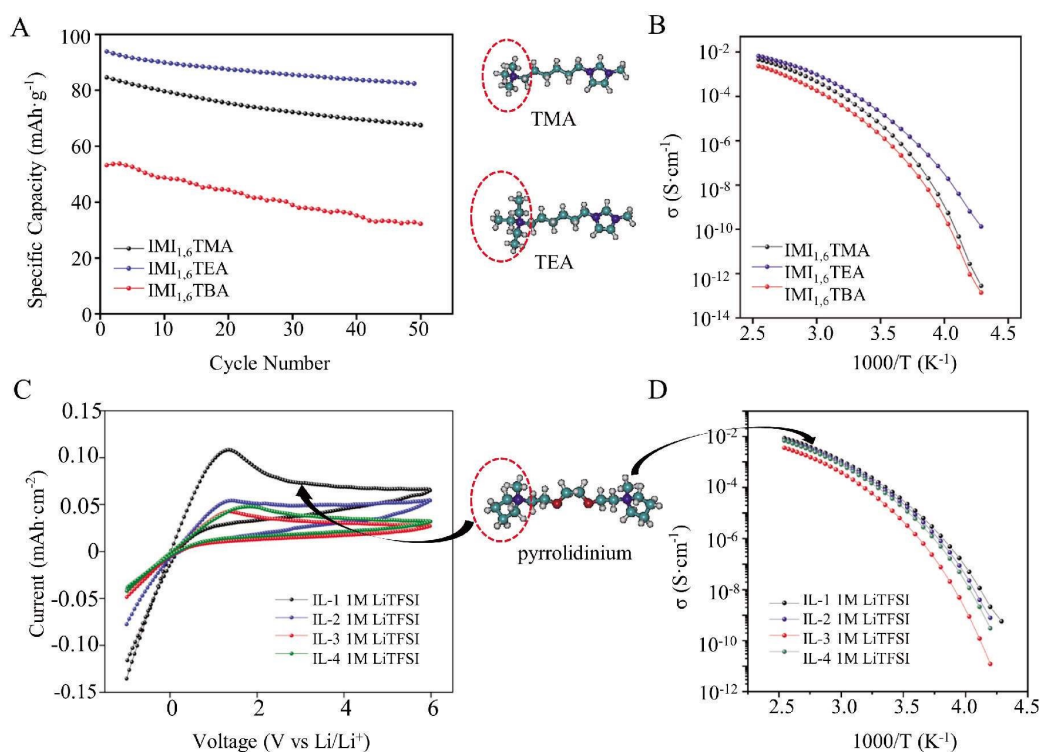**Figure 11** (A) Conductivity as a function of temperature for asymmetrical DILs $[C_6(tma)(mim)][Tf_2N]_2$ (IMI$_{1,6}$TMA), $[C_6(tea)(mim)][Tf_2N]_2$ (IMI$_{1,6}$TEA) and $[C_6(tba)(mim)][Tf_2N]_2$ (IMI$_{1,6}$TBA) electrolytes in LIBs. Reproduced with permission of Ref. 77, Copyright 2018, Elsevier. (B) Cycling performance of LIBs with asymmetrical DILs electrolytes. Reproduced with permission of Ref. 77, Copyright 2018, Elsevier. (C) Influences of the dicationic head type and spacer length on the operating voltage window. Reproduced with permission of Ref. 53, Copyright 2019, Elsevier. (D) Influences of the dicationic head type and spacer length on the conductivity-time function for LIBs in electrolytes pyrrolidinium DILs with two ether units spacer (IL-1) and three ether units spacer (IL-2), and piperidinium DILs with two ether units spacer (IL-3) and three ether units spacer (IL-4). Reproduced with permission of Ref. 53, Copyright 2019, Elsevier. (color on line)

MILs electrolytes and PILs electrolytes, OILs electrolytes show similar or even larger operating voltages and the more superior capacitive performance for supercapacitors with various electrode materials (such as graphene, CNT, and OLC) and LIBs. Moreover, the ionic delivery of OILs is poorer than that of MILs but far greater than that of gel or solid PILs, furtherly, incorporating proper organic solvents can make OILs maintain high mobility and effectively supply the gap of power performance between OILs and MILs. In addition, OILs can be applied under lower temperatures compared with PILs, ensuring the safety of LIBs at room temperature. Hence, OILs electrolytes own enormous potential in supercapacitors and LIBs.

4 Future Directions for Research

According to the reported work, OILs-based electrolytes are booming to meet the growing needs of high-performance energy storage systems such as supercapacitors and LIBs, stemming from their more tunable and prominent electrochemical properties. Designing OILs electrolytes reasonably in accordance with certain working conditions and requirements is imperative. Although great progress probing the relations of different characteristics and structures for OILs together with the OILs electrolytes/electrodes interfaces for supercapacitors and LIBs have been made, some challenges remain to be settled for academic researches or practical applications:

(1) Modeling can provide powerful theoretical support for macro-experiments to optimize or design OILs with promising physical chemistry properties in specific applications. Precise force fields are core factors in revealing the relations between microstructures and physicochemical characteristics in MD simulations. The force fields with a charge scale factor for OILs can resoundingly predict physical and structural properties, and the errors between the obtained ionic kinetic qualities and experimental data are within acceptable limits[57, 80]. However, in contrast to non-polarized force fields, the polarized ones effectively highlight associations between ions, which is inescapable for quite high-viscosity OILs[67]. There-

fore, it is necessary to focus on the establishment of the non-polarized force field with higher accuracy and lower calculational expense for OILs, especially for ether-spacer OILs owing to smaller viscosities and wider working voltage windows compared with alkyl chain-spacer ones[60]. In turn, the more comprehensive properties (Table 2 and Table 3) of the existing OILs and *C-V* curves of OILs/carbon electrodes EDLs in macro-experiments are needed to verify the accuracy of simulations.

(2) Properties of OILs depend on their structures, thus, OILs electrolytes with certain properties (such as melting point, thermostability, viscosity, and electrochemical stability) can be designed to match the practical requirements of supercapacitors and LIBs by adjusting molecular structures. For example, lowering the melting point of OILs by increasing the spacer length between rings or replacing other anions with [Tf$_2$N$^-$] and elevating the thermostability by weakening cationic symmetry can make supercapacitors and LIBs work safely at extreme temperatures. Moreover, extending the length of the spacers and shortening the side chains in multications can gain faster ionic mobility and higher power density for supercapacitors and LIBs. In addition, introducing the ether-based spacer and ammonium groups to cations in OILs can generate quite wide voltage windows, which helps to obtain greater energy density of OILs-based supercapacitors and LIBs.

(3) Furtherly, it is crucial to match the electrolyte and the designated electrode for supercapacitors. Currently, the electrodes of supercapacitors with OILs electrolytes are almost composed of multilayer graphene. However, nanopore electrodes are also considered up-and-coming candidates, due to the broad occupied surface area and the priority ability of the charge transport. For this reason, the working mechanism of OILs/nanopore electrode EDLs and the role of pore sizes should be further investigated to design new outstanding supercapacitors.

(4) In practical applications, OILs can absorb water from humid surroundings regardless of hydrophilic and hydrophobic characteristics. For this

reason, many works have been conducted to investigate bulk structures and internal interactions of water/OIL solutions. Unfortunately, water in OILs will undergo electrolytic reactions on the electrodes, significantly shrinking the operating voltage windows and blocking ionic valid progress for energy-storage devices such as supercapacitors and LIBs. Thus, figuring out the arrangement of water and ions at the humid OILs/electrode interfaces is necessary. Moreover, to save the expenses of OILs production at scale and remove impurities maximally in industrial engineering, there is an urgent need to develop more advanced preparative techniques.

(5) On the other side, organic solvents as additives of viscous OILs electrolytes are flammable, which is unfavorable for the safe usage of supercapacitors. Previous studies have shown that mixing organic solvents with an appropriate amount of water can drop flash points in the mixtures, thereby, avoiding the risk of burning and explosion[94]. Therefore, to gain safe supercapacitors with excellent power and energy density, cheap water can be added to OILs/organic solvents as ternary electrolytes, which can reuse impurity water in OILs and dramatically cut the production cost of great-performance supercapacitors. Today, this topic remains unrevealed. It is important to inspect the structural and capacitive behaviors of EDLs with ternary electrolytes especially the adsorption of water on the electrodes, helping to seek the optimal proportion of three substances in the hybrid electrolyte OIL/ACN/water.

(6) Finally, to satisfy the specific industrial need, realizing the high voltage windows and rapid ion motions of the OILs electrolytes under extreme environments is still challenging research. Up to now, OILs-based electrolytes for supercapacitors and LIBs are mainly confined to academic research, it is still a very long way before they can be put into practical applications at scale.

References:

[1] Koohi-Fayegh S, Rosen M A. A review of energy storage types, applications and recent developments[J]. J. Energy Storage, 2020, 27: 101047.

[2] Abbas Q, Mirzaeian M, Hunt M R C, Hall P, Raza R. Current state and future prospects for electrochemical energy storage and conversion systems[J]. Energies, 2020, 13(21): 5847.

[3] Behabtu H A, Messagie M, Coosemans T, Berecibar M, Anlay Fante K, Kebede A A, Mierlo J V. A review of energy storage technologies' application potentials in renewable energy sources grid integration[J]. Sustainability, 2020, 12(24): 10511.

[4] Simon P, Gogotsi Y, Dunn B. Where do batteries end and supercapacitors begin?[J]. Science, 2014, 343: 1210-1211.

[5] Yang Y S. A review of electrochemical energy storage researches in the past 22 years[J]. J. Electrochem., 2020, 26(4): 443-463.

[6] Daud M Z, Mohamed A, Hannan M A. An improved control method of battery energy storage system for hourly dispatch of photovoltaic power sources[J]. Energy Convers. Manage., 2013, 73: 256-270.

[7] Hannan M A, Lipu M, Hussain A, Mohamed A. A review of lithium-ion battery state of charge estimation and management system in electric vehicle applications: challenges and recommendations[J]. Renew. Sustain Energy Rev., 2017, 78: 834-854.

[8] Niu H Z, Wang L, Guan P, Zhang N, Yan C R, Ding M L, Guo X L, Huang T T, Hu X L. Recent advances in application of ionic liquids in electrolyte of lithium ion batteries [J]. J. Energy Storage, 2021, 40: 102659.

[9] Arbizzani C, Gabrielli G, Mastragostino M. Thermal stability and flammability of electrolytes for lithium-ion batteries[J]. J. Power Sources, 2011, 196(10): 4801-4805.

[10] Lin X, Salari M, Arava L M R, Ajayan P M, Grinstaff M W. High temperature electrical energy storage: Advances, challenges, and frontiers[J]. Chem. Soc. Rev., 2016, 45

(21): 5848-5887.

[11] Wang Q S, Jiang L H, Yu Y, Sun J H. Progress of enhancing the safety of lithium ion battery from the electrolyte aspect[J]. Nano Energy, 2019, 55: 93-114.

[12] Huang S F, Zhu X L, Sarkar S, Zhao Y F. Challenges and opportunities for supercapacitors[J]. APL Mater., 2019, 7 (10): 100901.

[13] Chen Y Q, Kang Y Q, Zhao Y, Wang L, Liu J L, Li Y X, Liang Z, He X M, Li X, Tavajohi N, Li B H. A review of lithium-ion battery safety concerns: The issues, strategies, and testing standards[J]. J. Energy Chem., 2021, 59: 83-99.

[14] Zhang Q K, Zhang X Q, Yuan H, Huang J Q. Thermally stable and nonflammable electrolytes for lithium metal batteries: Progress and perspectives[J]. Small Science, 2021, 1(10): 2100058.

[15] Poonam, Sharma K, Arora A, Tripathi S K. Review of supercapacitors: Materials and devices[J]. J. Energy Storage, 2019, 21: 801-825.

[16] Sharma P, Kumar V. Current technology of supercapacitors: A review[J]. J. Electron. Mater., 2020, 49(6): 3520-3532.

[17] Horn M, MacLeod J, Liu M, Webb J, Motta N. Supercapacitors: A new source of power for electric cars?[J]. Econ. Anal. Policy, 2019, 61: 93-103.

[18] Wang R, Yao M J, Niu Z Q. Smart supercapacitors from materials to devices[J]. InfoMat, 2020, 2(1): 113-125.

[19] Ma H L, Zhang Y Y, Shen M H. Application and prospect of supercapacitors in internet of energy(IOE)[J]. J. Energy Storage, 2021, 44: 103299.

[20] Yang Y C, Han Y H, Jiang W K, Zhang Y Y, Xu Y M, Ahmed A M. Application of the supercapacitor for energy storage in china: Role and strategy[J]. Appl. Sci.-Basel, 2022, 12(1): 354.

[21] Wang Y G, Song Y F, Xia Y Y. Electrochemical capacitors: Mechanism, materials, systems, characterization and applications[J]. Chem. Soc. Rev., 2016, 45(21): 5925-5950.

[22] Miller J R, Simon P. Materials science. Electrochemical capacitors for energy management[J]. Science, 2008, 321 (5889): 651-652.

[23] Pal B, Yang S Y, Ramesh S, Thangadurai V, Jose R. Electrolyte selection for supercapacitive devices: A critical review[J]. Nanoscale Adv., 2019, 1(10): 3807-3835.

[24] Zhang J Y, Yao X H, Misra R K, Cai Q, Zhao Y L. Progress in electrolytes for beyond-lithium-ion batteries [J]. J. Mater. Sci. Technol., 2020, 44: 237-257.

[25] Tang X, Lv S Y, Jiang K, Zhou G H, Liu X M. Recent development of ionic liquid-based electrolytes in lithium-ion batteries[J]. J. Power Sources, 2022, 542: 231792.

[26] Yu L P, Chen G Z. Ionic liquid-based electrolytes for supercapacitor and supercapattery[J]. Front. Chem., 2019, 7: 272.

[27] Lauw Y, Horne M D, Rodopoulos T, Nelson A, Leermakers F A M. Electrical double-layer capacitance in room temperature ionic liquids: Ion-size and specific adsorption effects[J]. J. Phys. Chem. B, 2010, 114(34): 11149-11154.

[28] Lamperski S, Outhwaite C W, Bhuiyan L B. The electric double-layer differential capacitance at and near zero surface charge for a restricted primitive model electrolyte[J]. J. Phys. Chem. B, 2009, 113(26): 8925-8929.

[29] Pinilla C, Del Popolo M G, Kohanoff J, Lynden-Bell R M. Polarization relaxation in an ionic liquid confined between electrified walls[J]. J. Phys. Chem. B, 2007, 111(18): 4877-4884.

[30] Baldelli S. Surface structure at the ionic liquid-electrified metal interface[J]. Acc. Chem. Res., 2008, 41(3): 421-431.

[31] Wang Y L, Li B, Sarman S, Mocci F, Fayer M D. Microstructural and dynamical heterogeneities in ionic liquids [J]. Chem. Rev., 2020, 120: 5798-5877.

[32] Wang X H, Salari M, Jiang D E, Varela J C, Anasori B, Wesolowskl D J, Dai S, Grinstaff M W, Gogotsi Y. Electrode material-ionic liquid coupling for electrochemical energy storage[J]. Nat. Rev. Mater., 2020, 5(11): 787-808.

[33] Anderson J L, Ding R F, Ellern A, Armstrong D W. Structure and properties of high stability geminal dicationic ionic liquids[J]. J. Am. Chem. Soc., 2005, 127(2): 593-604.

[34] Liu Q B, Rantwijk F V, Sheldon R A. Synthesis and application of dicationic ionic liquids[J]. J. Chem. Technol. Biotechnol., 2006, 81: 401-405.

[35] Guglielmero L, Mezzetta A, Guazzelli L, Pomelli C S, D' Andrea F, Chiappe C. Systematic synthesis and properties evaluation of dicationic ionic liquids, and a glance into a potential new field[J]. Front. Chem., 2018, 6: 612.

[36] Bhatt D R, Maheria K C, Parikh J K. A microwave assisted one pot synthesis of novel ammonium based dicationic ionic liquids[J]. RSC Adv., 2015, 5(16): 12139-12143.

[37] Zhang Z X, Yang L, Luo S C, Tian M, Tachibana K, Kamijima K. Ionic liquids based on aliphatic tetraalkylammonium dications and TFSI anion as potential electrolytes[J]. J. Power Sources, 2007, 167: 217-222.

[38] Wang R, Jin C M, Twamley B, Shreeve J M. Syntheses and characterization of unsymmetric dicationic salts incorporating imidazolium and triazolium functionalities

[J]. Inorg. Chem., 2006, 45: 6396-6403.

[39] Payagala T, Huang J, Breitbach Z S, Sharma P S, Armstrong D W. Unsymmetrical dicationic ionic liquids: Manipuation of physicochemical properties using specific structural architectures[J]. Chem. Mater., 2007, 19: 5848-5850.

[40] Chang J C, Ho W Y, Sun I W, Tung Y L, Tsui M C, Wu T Y, Liang S S. Synthesis and characterization of dicationic ionic liquids that contain both hydrophilic and hydrophobic anions[J]. Tetrahedron, 2010, 66(32): 6150-6155.

[41] Brown P, Butts C P, Eastoe J, Hernandez E P, Machado F L D A, Oliveira R J D. Dication magnetic ionic liquids with tuneable heteroanions[J]. Chem. Commun., 2013, 49: 2765.

[42] Zhou N, Zhao G Y, Dong K, Sun J, Shao H W. Investigations on a series of novel ionic liquids containing the $[closo\text{-}B_{12}Cl_{12}]^{2-}$ dianion[J]. RSC Adv., 2012, 2: 9830-9838.

[43] Kuhn B L, Osmari B F, Heinen T M, Bonacorso HG, Zanatta N, Nielsen S O, Ranathunga D T S, Villetti M A, Frizzo C P. Dicationic imidazolium-based dicarboxylate ionic liquids: Thermophysical properties and solubility[J]. J. Mol. Liq., 2020, 308: 112983.

[44] Sharma P S, Payagala T, Wanigasekara E, Wijeratne A B, Huang J M, Armstrong D W. Trigonal tricationic ionic liquids: Molecular engineering of trications to control physicochemical properties[J]. Chem. Mater., 2008, 20(13): 4182-4184.

[45] Wanigasekara E, Zhang X T, Nanayakkara Y, Payagala T, Moon H, Armstrong D W. Linear tricationic room-temperature ionic liquids: Synthesis, physiochemical properties, and electrowetting properties[J]. ACS Appl. Mater. Interfaces, 2009, 1(10): 2126-2133.

[46] López F I, Ibarra-Sanchez L, Domínguez-Esquivel J M, Miranda-Olvera A D, Bravo R H, Lagunas-Rivera S. Experimental and theoretical study on the synthesis and thermophysical properties of newer tricationic ionic liquids[J]. J. Mol. Struct., 2022, 1263: 133164.

[47] Mogurampelly S, Keith J R, Ganesan V. Mechanisms underlying ion transport in polymerized ionic liquids[J]. J. Am. Chem. Soc., 2017, 139(28): 9511-9514.

[48] Yuan J, Mecerreyes D, Antonietti M. Poly(ionic liquid)s: An update[J]. Prog. Polym. Sci., 2013, 38(7): 1009-1036.

[49] Mecerreyes D. Polymeric ionic liquids: Broadening the properties and applications of polyelectrolytes[J]. Prog. Polym. Sci., 2011, 36(12): 1629-1648.

[50] Qian W, Texter J, Feng Y. Frontiers in poly(ionic liquid)s: Syntheses and applications[J]. Chem. Soc. Rev., 2017, 46.(4): 1124-1159

[51] Matsumoto M, Saito Y, Park C Y, Fukushima T, Aida T. Ultrahigh-throughput exfoliation of graphite into pristine 'single-layer' graphene using microwaves and molecularly engineered ionic liquids[J]. Nat. Chem., 2015, 7: 730-736.

[52] Matsumoto M, Shimizu S, Sotoike R, Watanabe M, Iwasa Y, Aida T. Exceptionally high electric double layer capacitances of oligomeric ionic liquids[J]. J. Am. Chem. Soc., 2017, 139(45): 16072-16075.

[53] Vélez J F, Vázquez-Santos M B, Amarilla J M, Herradón B, Morales E. Geminal pyrrolidinium and piperidinium dicationic ionic liquid electrolytes. Synthesis, characterization and cell performance in $LiMn_2O_4$ rechar geable lithium cells[J]. J. Power Sources, 2019, 439: 227098.

[54] Zhang Z X, Zhou H Y, Yang L, Tachibana K, Kamijima K, Jian X. Asymmetrical dicationic ionic liquids based on both imidazolium and aliphatic ammonium as potential electrolyte additives applied to lithium secondary batteries[J]. Electrochim. Acta, 2008, 53(14): 4833-4838.

[55] Li S, Zhu M Y, Feng G. The effects of dication symmetry on ionic liquid electrolytes in supercapacitors[J]. J. Phys.: Condens. Matter., 2016, 28: 464005.

[56] Li S, Feng G, Cummings P T. Interfaces of dicationic ionic liquids and graphene: a molecular dynamics simulation study[J]. J. Phys. Condens. Matter, 2014, 26(28): 284106.

[57] Li S, Van Aken K L, McDonough J K, Feng G, Gogotsi Y, Cummings P T. The electrical double layer of dicationic ionic liquids at onion-like carbon surface[J]. J. Phys. Chem. C, 2014, 118: 3901-3909.

[58] Costa R, Pereira C M, Silva A F. Dicationic ionic liquid: Insight in the electrical double layer structure at mercury, glassy carbon and gold surfaces[J]. Electrochim. Acta, 2014, 116: 306-313.

[59] Li D D, Yang Y R, Wang X D, Feng G. Electrical double layer of linear tricationic ionic liquids at graphite electrode[J]. J. Phys. Chem. C, 2020, 124: 15723-15729.

[60] Lian C, Su H, Liu H, Wu J Z. Electrochemical behavior of nanoporous supercapacitors with oligomeric ionic liquids[J]. J. Phys. Chem. C, 2018, 122(26): 14402-14407.

[61] Yeganegi S, Soltanabadi A, Farmanzadeh D. Molecular dynamic simulation of dicationic ionic liquids: Effects of anions and alkyl chain length on liquid structure and diffusion[J]. J. Phys. Chem. B, 2012, 116(37): 11517-11526.

[62] Farmanzadeh D, Soltanabadi A, Yeganegi S. DFT study of the geometrical and electronic structures of geminal dicationic ionic liquids 1,3-bis[3-methylimidazolium-1-yl] hexane halides[J]. J. Chin. Chem. Soc., 2013, 60(5): 551-558.

[63] Sedghamiz E, Khashei F, Moosavi M. Linear tricationic ionic liquids: Insights into the structural features using DFT and molecular dynamics simulation[J]. J. Mol. Liq., 2018, 271: 96-104.

[64] Lopes J N C, Padua A A H. Molecular force field for ionic liquids composed of triflate or bistriflylimide anions [J]. J. Phys. Chem. B, 2004, 108(43): 16893-16898.

[65] Li S, Feng G, Cummings P T. Interfaces of dicationic ionic liquids and graphene: A molecular dynamics simulation study[J]. J. Phys.: Condens. Matter, 2014, 26(28): 284106.

[66] Lopes J N C, Deschamps J, Padua A A H. Modeling ionic liquids using a systematic all-atom force field[J]. J. Phys. Chem. B, 2004, 108(6): 2038-2047.

[67] Sedghamiz E, Moosavi M. Tricationic ionic liquids: Structural and dynamical properties via molecular dynamics simulations[J]. J. Phys. Chem. B, 2017, 121(8): 1877-1892.

[68] Torkzadeh M, Moosavi M. Heterogeneity in microstructures and dynamics of dicationic ionic liquids with symmetric and asymmetric cations-sciencedirect[J]. J. Mol. Liq., 2021, 330: 115632.

[69] Bodo E, Chiricotto M, Caminiti R. Structure of geminal imidazolium bis(trifluoromethylsulfonyl)imide dicationic ionic liquids: A theoretical study of the liquid phase[J]. J. Phys. Chem. B, 2011, 115(49): 14341-14347.

[70] Khakan H, Yeganegi S. Molecular dynamics simulations of amide functionalized imidazolium bis(trifluoromethanesulfonyl)imide dicationic ionic liquids[J]. J. Phys. Chem. B, 2017, 121(31): 7455-7463.

[71] Prado C E R, Freitas L C G. Molecular dynamics simulation of the room-temperature ionic liquid 1-butyl-3-methylimidazolium tetrafluoroborate[J]. Theochem-J. Mol. Struct., 2007, 847(1-3): 93-100.

[72] Tariq M, Forte P A S, Costa Gomes M F, Canongia Lopes J N, Rebelo L P N. Densities and refractive indices of imidazolium and phosphonium based ionic liquids: Effect of temperature, alkyl chain length and anion[J]. J. Chem. Thermodyn., 2009, 41(6): 790-798.

[73] Mahapatra A, Chakraborty M, Barik S, Sarkar M. Comparison between pyrrolidinium-based and imidazolium-based dicationic ionic liquids: Intermolecular interaction, structural organization, and solute dynamics[J]. Phys. Chem. Chem. Phys., 2021, 23: 21029.

[74] Moosavi M, Khashei F, Sharifi A, Mirzaei M. Transport properties of short alkyl chain length dicationic ionic liquids—the effects of alkyl chain length and temperature [J]. Ind. Eng. Chem. Res., 2016, 55(33): 9087-9099.

[75] Ishida T, Shirota H. Dicationic versus monocationic ionic liquids: Distinctive ionic dynamics and dynamical heterogeneity[J]. J. Phys. Chem. B, 2013, 117(4): 1136-1150.

[76] Chatterjee K, Pathak A D, Lakma A, Sharma C S, Singh A K. Synthesis, characterization and application of a non-flammable dicationic ionic liquid in lithium-ion battery as electrolyte additive[J]. Sci. Rep., 2020, 10(1): 9606.

[77] Vélez J F, Vazquez-Santos M B, Amarilla J M, Tartaj P, Morales E. Asymmetrical imidazolium-trialkylammonium room temperature dicationic ionic liquid electrolytes for Li-ion batteries[J]. Electrochim. Acta, 2018, 280: 171-180.

[78] Hossein H, Gildeh S F G, Ghauri K, Fathei P. Physicochemical properties of the imidazolium-based dicationic ionic liquids (DILs) composed of ethylene π-spacer by changing the anions: A quantum chemical approach[J]. Ionics, 2020, 26: 1963-1988.

[79] Yeganegi S, Sokhanvaran V, Soltanabadi A. Study of thermodynamic properties of imidazolium-based ionic liquids and investigation of the alkyl chain length effect by molecular dynamics simulation[J]. Mol. Simul., 2013, 39(13): 1070-1078.

[80] Li D D, Li E C, Yang Y R, Wang X D, Feng G. Structure and capacitance of electrical double layers in tricationic ionic liquids with organic solvents[J]. J. Phys. Chem. B, 2021, 125(46): 12753-12762.

[81] Sun H, Zhang D J, Liu C B, Zhang C Q. Geometrical and electronic structures of the dication and ion pair in the geminal dicationic ionic liquid 1,3-bis [3-methylimidazolium-yl]propane bromide[J]. Theochem-J. Mol. Struct., 2009, 900(1-3): 37-43.

[82] Alavi S M, Yeganegi S. Computational study of halogen-free boron based dicationic ionic liquids of [bis-mim] [bmb]₂ and [bis-mim][bscb]₂[J]. Spectrochim. Acta, Part A, 2019, 210: 181-192.

[83] Li S, Feng G, Bañuelos J L, Rother G, Fulvio P F, Dai S, Cummings P T. Distinctive nanoscale organization of dicationic versus monocationic ionic liquids[J]. J. Phys. Chem. C, 2013, 117(35): 18251-18257.

[84] Li S, Bañuelos J L, Zhang P F, Feng G, Dai S, Rother G, Cummings P T. Toward understanding the structural heterogeneity and ion pair stability in dicationic ionic liquids [J]. Soft Matter, 2014, 10(45): 9193-9200.

[85] Torkzadeh M, Moosavi M. Probing the effect of side alkyl chain length on the structural and dynamical micro-heterogeneities in dicationic ionic liquids[J]. J. Phys. Chem. B, 2020, 124(50): 11446-11462.

[86] Serva A, Migliorati V, Lapi A, Aquilanti G, Arcovito A,

D'Angelo P. Structural properties of geminal dicationic ionic liquid/water mixtures: A theoretical and experimental insight[J]. Phys. Chem. Chem. Phys., 2016, 18(24): 16544-16554.

[87] Bhargava B L, Klein M L. Nanoscale organization in aqueous dicationic ionic liquid solutions[J]. J. Phys. Chem. B, 2011, 115(35): 10439.

[88] Bhargava B L, Klein M L. Formation of interconnected aggregates in aqueous dicationic ionic liquid solutions[J]. J. Chem. Theory Comput., 2010, 6(3): 873.

[89] Palchowdhury S, Bhargava B L. Effect of spacer chain length on the liquid structure of aqueous dicationic ionic liquid solutions: Molecular dynamics studies[J]. Phys. Chem. Chem. Phys., 2015, 17(17): 11627-11637.

[90] Li S, Feng G, Cummings P T. The effects of dication symmetry on ionic liquid electrolytes in supercapacitors [J]. J. Phys.: Condens. Matter, 2016, 28: 464005.

[91] Li S, Zhang P, Pasquale F F, Patrick C H, Feng G, Dai S, Peter T C. Enhanced performance of dicationic ionic liquid electrolytes by organic solvents[J]. J. Phys. Condens. Matter, 2014, 26(28): 284105.

[92] Wagner R, Preschitschek N, Passerini S, Leker J, Winter M. Current research trends and prospects among the various materials and designs used in lithium-based batteries [J]. J. Appl. Electrochem., 2013, 43: 481-496.

[93] Vélez J F, Santos M B V, Amarilla J M, Herradón B, Morales E. Geminal pyrrolidinium and piperidinium dicationic ionic liquid electrolytes. Synthesis, characterization and cell performance in LiMn$_2$O$_4$ rechargeable lithium cells[J]. J. Power Sources, 2019, 439: 227098.

[94] Xiao D W, Dou Q Y, Zhang L, Ma Y L, Shi S Q, Lei S L, Yu H Y, Yan X B. Optimization of organic/water hybrid electrolytes for high-rate carbon-based supercapacitor[J]. Adv. Funct. Mater., 2019, 29(42): 1904136.

低聚离子液体的体相与界面及其电化学储能应用

李丹丹[1,2]，纪翔宇[3]，陈　明[3]，杨燕茹[1,2]，王晓东[1,2*]，冯　光[3*]

(1. 华北电力大学可再生能源替代电力系统国家重点实验室, 北京 102206；2. 华北电力大学工程热物理研究中心, 北京 102206；3. 华中科技大学能源与动力工程学院, 燃煤国家重点实验室, 湖北 武汉 430074)

摘要： 近年来，随着单阳离子液体的发展，新型低聚物离子液体被合成并应用。这类离子液体可看作是由几个重复的单阳离子组合而成，可以通过改变阳离子带电基团、间隔连接的长度或种类、末端链的长度以及阴离子种类来获得更多不同的结构。因此，低聚离子液体有更复杂的微观结构和内部相互作用，决定了其多特征的物化性质和电化学特性，有望满足更多对溶剂性能有特定要求的应用。例如，与单阳离子液体相比，低聚离子液体具有更大的可调节性、更宽的液态温度范围、更高的热稳定性等优点，使其在电化学储能设备中得到越来越多的应用，如用作超级电容器和锂离子电池的电解液。在本综述中，我们系统地总结并详细解释了低聚离子液体的性质和结构（包括单个离子的结构和本体液内部的纳米组织）之间的关联，主要是双阳离子液体和三阳离子液体；概括了低聚离子液体作为超级电容器和锂离子电池的电解液的相关研究，重点阐述了由低聚离子液体和不同类型电极组成的双电层的结构和性能，以及与相应单阳离子液体电解液的比较结果；提供了降低低聚离子液体粘度和加速离子扩散的优化措施，提出了低聚离子液体电解液未来可能面临的主要问题和发展前景。

关键词： 聚离子液体；性质和结构；超级电容器；锂离子电池